Aus der Klinik für **Angeborene Herzfehler und Kinderkardiologie**

der Medizinischen Fakultät Charité – Universitätsmedizin Berlin

DISSERTATION

Detection of dose-dependent effects of the β-blocker Esmolol on myocardial deformation using MRI-tagging

zur Erlangung des akademischen Grades

Doctor medicinae (Dr. med.)

vorgelegt der Medizinischen Fakultät

Charité – Universitätsmedizin Berlin

von

Tieyan Li / 李铁岩

aus **Shenyang, Liaoning Province, P. R. China**

Gutachter: 1. Prof. Dr. med. F. Berger

2. Prof. Dr. med. S. Dittrich

3. Priv.-Doz. Dr. med. U. Teichgräber

Datum der Promotion: 04.12.2012

Catalogue

1 Introduction
1.1 Background ---------- 1
1.2 Myocardium Architecture ---------- 2
1.3 Magnetic Resonance Tagging ---------- 8
1.4 β-blocker ---------- 12

2 Hypothesis ---------- 15

3 Material and Methods
3.1 Study Population ---------- 16
3.2 Volunteers Preparation ---------- 16
3.3 MRI Sequence Parameters ---------- 16
3.4 CSPAMM Technique (Complementary Spatial Modulation of Magnetization) ---------- 17
3.5 MRI Tagging Protocol ---------- 17
3.6 MRI Tagging Image Analysis ---------- 18
3.7 Statistics ---------- 21

4 Results
4.1 Curve analysis ---------- 22
4.1.1 Circumferential Shortening (CS) ---------- 23
4.1.2 Radial Shortening (RS) ---------- 25
4.1.3 Rotation ---------- 25
4.1.4 Longitudinal Shortening (LS) ---------- 26
4.2 Statistics analysis on effect on myocardium with different doses of β-blocker ---------- 27
4.2.1 Circumferential Shortening (CS) ---------- 27
4.2.2 Radial Shortening (RS) ---------- 30
4.2.3 Rotation ---------- 33
4.2.4 Longitudinal Shortening (LS) ---------- 36

5 Discussion
5.1 Interpretation of the study results ---------- 38
5.2 MRI tagging ---------- 40
5.2.1 The advantages of MRI Tagging ---------- 40
5.2.2 Comparison with other clinical imaging modalities to display myocardial motion ---------- 42
5.2.3 Technical considerations to improve MRI tagging ---------- 43
5.2.4 HARP ---------- 44
5.3 β-blockers ---------- 45
5.3.1 Mechanisms of β-blocker action ---------- 46
5.3.2 The characters of β-blockers Esmolol ---------- 47
5.3.3 Detection of benefit of low doses of β-blocker Esmolol from our study ---------- 48
5.3.4 Support from clinical reports ---------- 50
5.4 Age ---------- 52
5.5 Gender ---------- 53

6 Summary ---------- 56
7 Literature ---------- 58
8 Figure list ---------- 64
9 Curriculum vitae ---------- 65
10 Statement in lieu of oath ---------- 66
11 Acknowledgement ---------- 67
12 Zusammenfassung (in German) ---------- 68

1 Introduction

1.1 Background

Myocardial dysfunction is a main disease in elder people. It can lead to heart failure (HF) which continues to be a major cause of morbidity and mortality in developed countries and in developing countries. Heart failure is a growing health problem worldwide. In America, the American Heart Association estimates that nearly 5.3 million Americans suffer from heart failure and that 283,000 annually die of heart disease (1). Its prevalence also continues to increase with aging of population. After initial hospitalization for heart failure, a staggering 22% 1-year mortality is evident. Coronary artery disease (CAD) is by far the most common cause of HF and accounts for approximately 70% of cases (2). In most of these patients an acute myocardial infarction (AMI) precedes the development of HF usually over several years as a result of the ischaemic myocardial injury.

The ischaemic injury triggers a series of adaptive mechanisms leading to changes in size, geometry, and function of the left ventricle (LV). This process, known as LV remodelling, is usually slow and may remain silent in clinic until symptoms of HF develop (2).

Regarding myocardial architecture, we consider that the LV myocardium consists of circumferential fibers in the mid-wall layer and longitudinal fibers in the endocardial and epicardial layers, and that myofiber orientation changes continuously from right-handed helix in subendocardium to left-handed helix in subepicardium (3). The LV function is determined by the sum of contraction and relaxation in these 3 layers. In fact the overall anatomic structure of the ventricle is a three-dimensional mesh with individual myocytes which aggregate by their long axes either running tangentially or obliquely relative to the thickness of the ventricular wall and set in a matrix of fibrous tissue (4). The matrix of fibrous tissue is called extracellular martrix (ECM) and consists of components like collagen I, III, IV, laminin and fibronectin.

As mentioned before in response to heart failure, the left ventricle undergoes structural and functional adaptations that collectively have been termed as LV remodelling. The remodelling is characterized by a structural rearrangement of the cardiac chambers that involves myocyte hypertrophy, fibroblast proliferation and an increased deposition of ECM. During LV remodelling, both ECM degradation and synthesis increase occur (5). When ECM degradation dominates over synthesis, LV rupture can occur. When ECM synthesis dominates over degradation rates, fibrosis can occur. Fibrosis increases myocardial stiffness and further depresses LV function to culminate in heart failure. The ventricular remodelling initiates a series of events beginning with increased wall stress, afterload mismatch, episodic subendocardial

hypoperfusion, increased oxygen utilization, increased oxidative stress and more (6). It further influences the myocardial movement and LV function as well as hemodynamics.

Heart failure further is characterized by changes in many neurohormonal mechanisms, but most notably by activation of the sympathetic and renin–angiotensin–aldosterone system. Inhibition of these two systems is the mainstay of current treatment. The prognosis for patients with heart failure has improved over recent decades, with the development and introduction of drugs such as angiotensin converting enzyme (ACE) inhibitors, angiotensin II receptor blockers (ARBII), aldosterone antagonists and β-blockers (7). Over the last three decades, the position of β-blockers has evolved from contraindication to established treatment. β-blockers have been shown to be of high benefit on reducing adrenergic drive, improving autonomic balance, reducing ventricular wall stress, prolonging diastole, reducing heart rate and increasing coronary perfusion time. Several large randomized trials and meta-analysis have presented that in patients with a low ejection fraction, β-blockers reduce hospital admissions for worsening heart failure and the risk of death by 30% (8). β-blockers are also a commonly prescribed class of medications that are known to improve the outcomes of patients with LV systolic dysfunction (9). β-blockers show significant results: easing symptoms, improving LV function and remodelling with reverse of heart failure and increase of survival.

When the heart suffers from ischaemic disease, there are many methods to detect the heart function, the movement and any other change of the heart or myocardium. But magnetic resonance image tagging is a valuable way to noninvasively assess local motion characteristics of the heart. As a valuable alternative to invasive implantation of radiopaque markers or the tracking of coronary bifurcations on cine x-ray coronary angiograms, myocardial tagging with magnetic resonance has been shown to be a very sensitive method for the assessment of the local contraction and relaxation pattern of the myocardium in healthy and diseased states. The Complementary Spatial Modulation of Magnetization (CSPAMM) is a magnetic resonance tagging method which can be applied for the acquisition and quantification of myocardial motion successfully. It noninvasively supports a 3D description of myocardial motion allowing conclusion on 3D myocytes architecture. Further more we can diagnose heart disease or assess the effect of the treatment.

1.2 Myocardial Architecture

The precise 3D architecture, the arrangement of the myocytes, is complex. Previous investigations have shown that there are countless small planes of cleavage interspersed throughout the myocardium, which facilitate relative movement between adjacent myocardial

aggregates, thus easing their rearrangement during systolic contraction and diastolic relaxation (10). Histology has furthermore established that, despite the highly interlaced nature of the ventricular myocardium, there are numerous local heterogeneities in the orientation and connections of the myocardial aggregates making up the ventricular wall. But it is exceedingly difficult to reconstruct the packing of the myocytes especially for reproducing the overall 3D architectural arrangement.

Anatomists have shown in numerous previous studies that the myocardium is arranged as anisotropic continuum, with the individual myocytes aligning in series and coupling to their neighbours through multiple offsprings, the overall mesh being supported by a matrix of connective tissue (4). The individual myocytes are attached one to the other when examined histologically. The aggregated myocytes can be displayed in an anatomically systematic sequence, starting from the base of the intact ventricle following the global arrangement. Their activity produces peristaltic movement along the lumens of the organs, with their speed of discharge being influenced by the autonomic nervous system. In order to ensure harmonic atrial and ventricular activity, each myocyte within the heart must not only conduct the impulse, but also contract at the right moment, at the appropriate speed, and to the necessary degree. It is the fashion in which the ventricular myocytes are arranged that produces the coordinated systolic contraction.

History: In the beginning the assumption was that the arrangement of the myocardial ‘grain’ in and out of the ventricular mass was organized in helical structure detected by Senac. In the 20th century the scientists realised that the ventricles were not arranged in the fashion of skeletal muscles, even if it was possible to discern apparent “tracts”, because the heart was in essence a modified blood vessel. In the late 1960s, ignoring the multiple anatomical studies which, over the centuries, had shown that the ventricular myocardium was arranged in the form of a modified blood vessel, the Spanish general practitioner Torrent-Guasp (10) dissected the ventricular myocardial mass, claiming to follow the perceived predominant longitudinal orientation of myocardial aggregates. However he ignored the essential that the dissector seeking to follow the course of myocardial aggregates through the ventricular walls must destroy the essential spatially netted nature of the ventricular myocardium. Frank’s group had presumed that all the aggregates were aligned more or less in the tangential plane. The ventricular cavities encircles in helical fashion. Until now Frank’s thesis is also a typical model of the arrangement of myocytes. Anderson’s research (11) proved that the outer and the endocardial components of the ventricular walls were made up primarily of aggregates aligned essentially tangentially to a virtual surface plane (Fig.1.2.1.a-b). The prevailing mass of myocytes aggregated with their long axes

tangentially relative to the thickness of the ventricular walls, is responsible for an over constriction of the ventricular cavity.

Fig.1.2.1.a

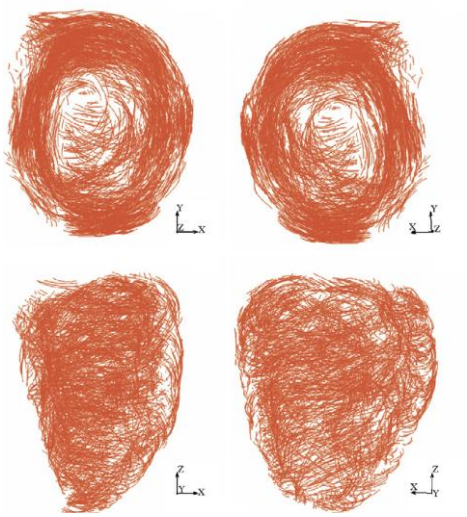

Fig.1.2.1.b

Fig.1.2.1.a The figure shows the reconstruction of the porcine LV with magnetic resonance diffusion tensor imaging. From here one can see the track of myocardium and see the arrangement of myocytes. (Anderson, How are the myocytes aggregated. Semin Thorac Cardiovasc Surg Pediatr Card Surg Ann. 2007)

Fig.1.2.1.b The figure shows a series of reconstructions of the myocardial aggregates progressively removed from the wall of a human LV, while the two upper panels of show the circular arrangement of the aggregates at the base of the LV. (Farshad, An analysis of the spatial arrangement of the myocardial aggregates making up the wall of the left ventricle. European Journal of Cardio-thoracic Surgery. 2007).

The myocytes within the heart, in terms of individual structure, also show cross-striations such as those seen in skeletal myocytes. The overall orientation of the long axis of the myocytes permits the distinction of circular as opposed to longitudinal layers within the walls of many of the organs or vessels, the long axis of the aggregated individual myocytes determining the overall orientation of the muscular layers.

The epicardial and the endocardial ‘fibers’ of the ventricular wall are made up primarily of myocytes orientated with the angles of their long axis almost at 90° to each other when they are measured relative to the equatorial plane as represented by the ventricular groove (4). When these angles relative to the equatorial plane are assessed at various depths within the wall, a gradation is seen in the angles relative to the ventricular equator. This is the so-called helical angle (Figure 1.2.2.b). In more details, when the superficial covering of myocytes is stripped away to reveal the middle and subendocardial portions, the subendocardial myocytes are arranged in a right-handed helix and the subepicardial myocytes in a left-handed helix. It is also to confirm that the helical angle of the subendocardial zones, as seen from the base to apex,

increases markedly in a clockwise fashion. When traced from the apex to the base, the angles of the subepicardial aggregates ascend in an anticlockwise fashion. By performing histologic analysis of the various parts of the ventricular walls and measuring the angles of the long axis of the myocytes aggregated within the various depths of the ventricular walls, the results show that the so-called helix angle changes markedly at different depths within the wall. The mean helical angles of the aggregates range from around +85° at the subendocardial surface to -85° at the subepicardial surface (Fig.1.2.2.a-b).

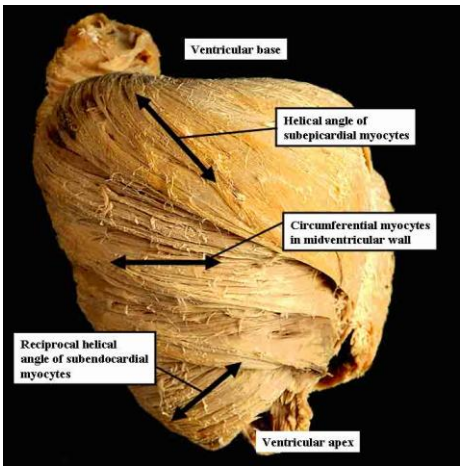

Fig.1.2.2.a

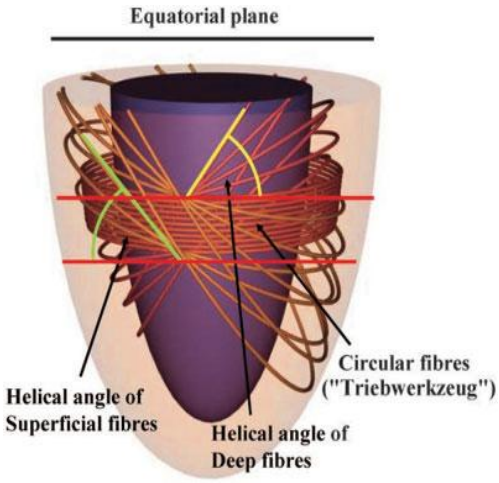

Fig.1.2.2.b

Fig.1.2.2.a This porcine heart has been dissected by stripping away within various depths of the ventricular wall. It shows the changing angles of the long axis of the aggregated myocytes in the different depths.

Fig.1.2.2.b The cartoon shows the variation in angles of the long axis of the aggregated myocytes when assessed relative to the ventricular equator. This is the so-called helical angles. (R.H.Anderson, Heuristic problems in defining the three-dimensional arrangement of the ventricular myocytes. Anat Rec Part A. 2006)

The arrangement of myocytes is homogeneous. The majority of the myocytes forming the myocardium are aggregated tangentially. Marked heterogeneity is found in terms of angles of the myocytes relative both to the equator of the left ventricle and to the epicardial surface lining. The most prominent aberration is seen at the apical vortex. But histology has furthermore detected that despite the highly interlaced nature of the ventricular myocardium there are numerous local heterogeneities in the orientation and connections of the myocardial aggregates making up the ventricular wall. By cutting semicircular full-thickness transmural sections from the ventricular walls to reveal an orderly array of longitudinal aggregates throughout the wall, significant numbers of aggregating myocytes deviate markedly from a tangential plane (4). Further obvious deviations from the purported tangential alignment of the myocytes are seen at the basal margins of both ventricles (12). In the whole heart, when aggregates are measured along their long axis, at the apex and at the base the deviation occurs in form of obliquely aggregated myocytes. These

myocytes show some change in orientation in radial fashion across the ventricular wall extending from epicardium to endocarium. These intruding oblique aggregates run throughout the circumference of the ventricular wall (11). Comparison between the septum and the free wall reveals more pronounced angles of intrusion in the septum, particularly at the junctions with the free wall. The inferior wall is densely interspersed with short segments oriented obliquely towards the endocardium. They are the intruding aggregated myocytes which are inclined up to 35° to the pericardial surface plane (12). These oblique myocytes are necessary to ensure the stability of the shape of the ventricular walls throughout their cyclical deformation. We think that they also constitute the major determinant of the cyclical realignment of the 3D arrangement of myocytes and thus are involved in diastolic reopening of the ventricle. The myocardial mass, however, as we have explained, is organized as a mesh of myocytes embedded in a scaffold of connective tissue. Mural thickening is part of an active process brought about by contraction, shortening, and thickening of the mesh and myocytes. When the heart contracts, the majority of the myocytes which are tangential will be responsible. While mural thickness increases, the tangential myocytes are erected in a radial direction with two adjacent rows of myocytes becoming three or four by alternate interleaving (13) (Fig.1.2.3). At the same time as mural thickening, the oblique transmural myocytes are progressively hindered in shortening. The result is that the myocytes which are aggregated with their long axis obliquely through the short axis of the wall can engender the auxotonic forces. This is opposite to the forces produced by the tangentially aggregated myocytes and provides balance for the entirety of the ventricular walls. In the normal heart, this population of obliquely orientated aggregates of myocytes has the function of attenuating the marked systolic mural ventricular thickening thus preserving the shape and size of the ventricular cavity. In the mid portion of the ventricular wall, deviations from an essentially tangential alignment were also found with the largest number of oblique aggregated myocytes located around the obtuse margin. And in particular adjacent to the ventricular base, the myocardial cells are oriented in a circular fashion forming the ‘triebwerkzeug’ (Fig.1.2.4).

But the oblique myocytes seem unlikely to be able to create enough force vector acting in the radial direction significant enough to induce ventricular diastolic dilation. First because the maximal deviation of these aggregates is not more than 45°, we believe that they need to work mutually with the supporting fibrous matrix so as to achieve the oblique deviation of forces which is required to control the amount and timing of regional mural thickening that is known to take place during systole (4). And second because their contractile mass is too small relative to the remainder of the mural myocardium. So we infer that any transmission of force in radial

direction requires the involvement of the connective tissue scaffold that supports the myocardial component of the mesh. When the myocardial ‘fibers’ shorten during systole, they also act on their supporting matrix of connective tissue. This scaffold then becomes part of the chain for transmission of spatial forces.

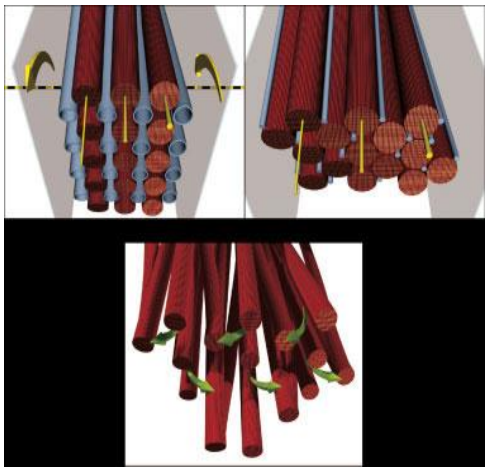

Fig.1.2.3

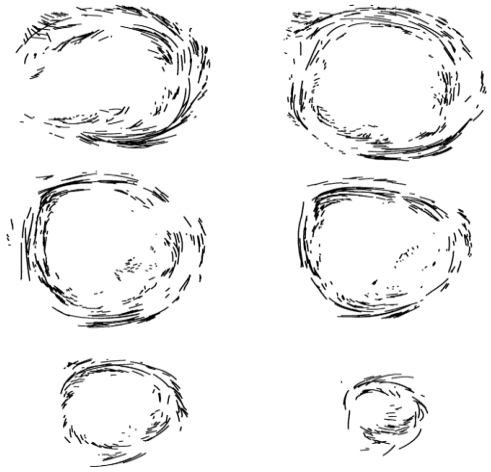

Fig.1.2.4

Fig.1.2.3 Realignment of an aggregate of myocytes and their accompanying capillaries from diastole (upper left) to systole (upper right), the lower one shows that in systolic mural thickening, the arrangement of myocytes in controlled by their off shoots which can enhance systolic myocardial thickening. (Lunkenheimer PP, The forces generated within the musculature of the left ventricular wall. Heart. 2004)

Fig.1.2.4 From the base to apical of the heart, the tangential orientations are predominant, but a marked local variability is seen in the angle of intrusion. The middle figures show the deformation of the cross-sections which deviate markedly from a circle.

The myocardium is a meshwork of myocytes set in a supporting matrix of fibrous tissue. The individual myocytes are packed together in the matrix which has endomysial, perimysial and epimysial components. The arrangement of the collagenous support is not such as to produce sheaths that separate the walls of the chambers in orderly fashion and the fibrous elements are also not fascial sheaths that permit each individual myocytes to be demonstrated in repetitive fashion. These myocytes are set in their supporting matrix, with irregular arrangements of thicker collagenous plates surrounding groups of myocytes and with various numbers of myocytes grouped together within different parts of the walls of the chambers (Fig.1.2.5.a-b). The only fibrous sheaths to be found within the overall muscular mass contained within the epicardium are those that insulate the ventricular conduction pathways from the adjacent ventricular myocardium. Because of these sheaths, the cardiac impulse, once having been delayed within the atrioventricular node, is rapidly disseminated to the apex of the ventricular mass so that ventricular contraction can expel the blood through the arterial trunks. Although the myocytes

are densely aggregated within the fibrous matrix, it is not possible to discern the striation representing their longitudinal orientation with the naked eye. This is because the angle between the trunk of myocytes and its offshoots is particularly small, so that a cursory gaze at the histologic appearance of the mesh might give the impression that all myocytes are running parallel, which is not the case.

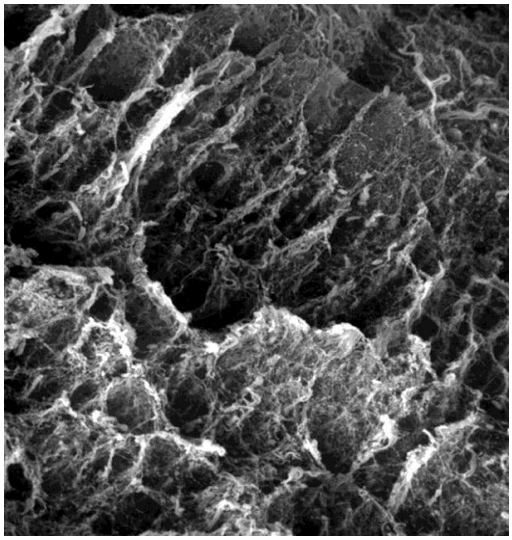

Fig.1.2.5.a

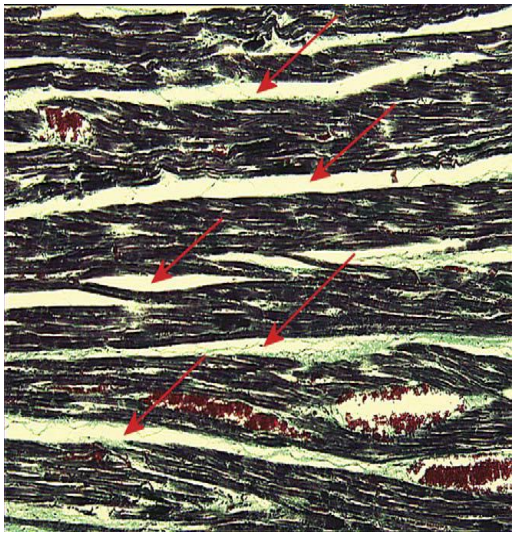

Fig.1.2.5.b

Fig.1.2.5.a This figure shows the arrangement of the fibrous tissue subsequent to digestion of the myocytes

Fig.1.2.5.b Histological section (magnification of 100 times) showing the ventricular myocytes supported by a fibrous matrix, with the myocytes stained dark, erythrocytes red, and supporting connective tissue green. (Lunkenheimer, The myocardium and its fibrous matrix working mutually as a spatially netted mesh: a critical review of the purported tertiary structure of the ventricular mass. European Journal of Cardio-thoracic Surgery. 2006)

1.3 Magnetic Resonance Tagging

Measures of global ventricular function and its reduced indices, such as ejection fraction, are clearly strong predictors of future of heart failure and poor prognosis. However, global measures are insensitive to reductions in regional performance, where even a normal ejection fraction can obscure significant underlying regional dysfunction (6). Many methods are used to detect the cardiac function and dysfunction. But there are also many limitations of the conventional methods used to assess cardiac function. Thus, measures of regional function, such as quantification of myocardial strain and torsion, have emerged as more accurate tools for defining degrees of myocardial disease. Traditional magnetic resonance (MR) techniques can provide information on global and regional wall motion but with limited spatial and temporal resolution. Doppler imaging and Speckle tracking are two novel echocardiographic techniques that have been introduced for strain quantification. While both techniques have demonstrated promising potential for bedside regional function assessment at a high temporal resolution (>250

frames/second), acquisition angle and operator dependence must be kept in mind while using these techniques. Some other methods to quantify myocardial function originally required invasive surgical implantation of physical markers within the myocardium and then tracking myocytes motion. However, this method is impractical for clinical application and implanted markers tend to influence cardiac motion and thus distort the accuracy of myocardial measurements (14). In 1988, Zerhouni (15) introduced a magnetic resonance based non-invasive imaging method for tracking myocardial motion: myocardial tissue tagging. Myocardial tagging is an MRI technique that can be used for quantitative assessment of myocardial function. It is an integrated approach which combines fast imaging pulse sequences, joint electrocardiogram (ECG) and respiratory gating, parallel imaging, and suitable cardiac coils may allow 3D tagging to be more practical. The basic idea of myocardial tagging was to create non-invasive markers within the myocardium by applying saturation planes perpendicular to the imaging plane with selective radiofrequency saturation of multiple thin tag planes at the ECG trigger signal before image acquisition. During the subsequent image acquisition, reduced signal is obtained from the saturated tissue. Therefore, the cut line of the image plane and the saturated plane appears as a hypointense or black line on the images (16) (Fig.1.3.1). With this MRI method, the myocardium dynamics can be studied noninvasively and without exposure to potentially harmful ionizing radiation.

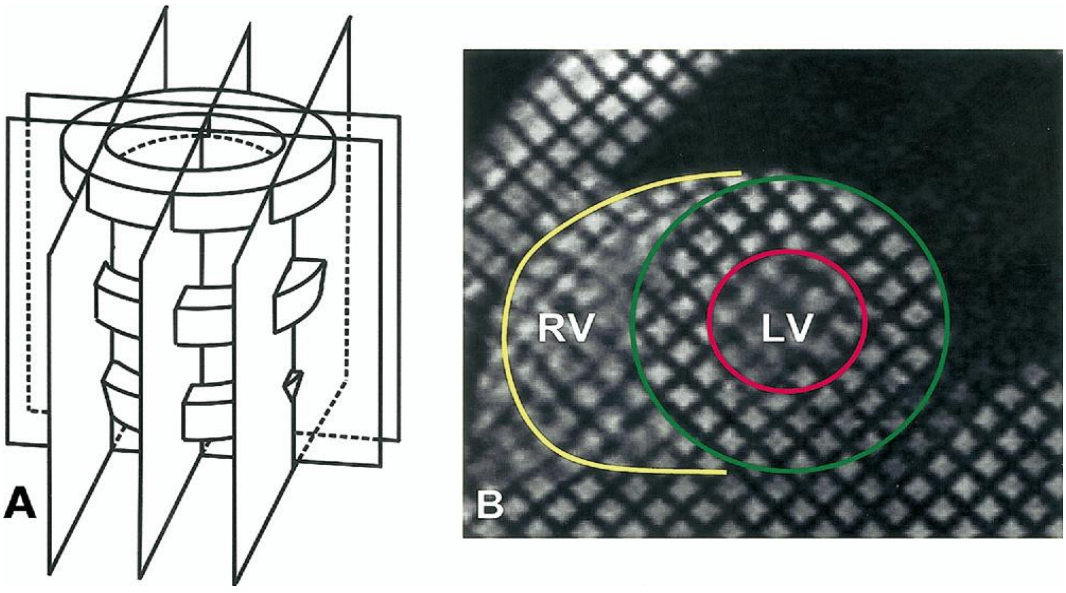

Fig.1.3.1 Basic principle of myocardial magnetic resonance tagging. The schematic drawing indicates the short-axis image planes and the magnetically saturated planes perpendicular to the imaging plane (A). During subsequent image acquisition, reduced signal is obtained from the saturated tissue. This results in black lines on the images (B). LV=left ventricle; RV=right ventricle. (Marco J. W. Götte, Myocardial Strain and Torsion Quantified by Cardiovascular Magnetic Resonance Tissue Tagging. Journal of the American College of Cardiolog. 2006)

The principle of myocardial tagging is based on producing a spatial pattern of saturated magnetization within the myocardium known as non-invasive markers-tagging at end diastole, and then imaging the resulting deformation of the pattern when the heart contracts through the cardiac cycle.

Some basic guidelines (14) for myocardial tagged MRI have become apparent:

1) The spatial resolution of the strain computed from the tagged images is nominally defined as the distance between two adjacent tags. Therefore, the spatial resolution of the imaging sequence must be able to provide at least two tags across the myocardial wall to assess radial strain.

2) The temporal resolution must be high enough to avoid motion blurring of tags. This condition is particularly important for tagging studies on diastolic dysfunction (e.g., the rapid filling phase of diastole) and myocardium motion abnormalities induced by pharmacologic stressors such as dobutamine which also increases the heart rate.

3) Pulse sequences with high data acquisition efficiency (e.g., spiral and EPI sample a large trajectory of k-space per RF excitation) produce higher tag contrast and longer tag persistence than conventional gradient echo sequences, but they are also more prone to sources of image artifacts such as static magnetic field inhomogeneity and motion.

The typical tagging is created upon detection of the QRS complex of the ECG. The resulting tagging follows the underlying myocardial deformation. However, fading of the tagging lines starts at end-diastole to the systolic part during the cardiac cycle because of tissue T1 relaxation and the imaging radiofrequency pulses. This fading may hamper assessment of regional myocardial function, especially the analysis of the relaxation of the heart during diastole. Using high field strength magnets for tagging acquisition may reduce the problem of tag fading. In fact, despite the potential increase in susceptibility effects during cardiac imaging, applying myocardial tagging at higher field strength appears to provide a better **c**ontrast to **n**oise **r**atio (CNR) as well as improve tag persistence. This could be attributed to a higher baseline **s**ignal to **n**oise **r**atio (SNR) provided by 3T systems and prolongation of myocardial T1, thus improving the contrast between the tissue and the tag lines at end-diastole. However, there are some other more effective methods to solve the problems such as applying multi-planar imaging. **C**omplementary **spa**tial **m**odulation of **m**agnetization (CSPAMM) is one of the MRI tagging technologies which can minimize the tag fading due to T1 relaxation and assess the whole heart. This technique acquires two tagged images based on **sp**atial **m**odulation of **m**agnetization (SPAMM) patterns that are 180 ° out of phase with each other and subtracts them with complementary signed tagging modulation (14). The subtraction technique reduces tagline intensity fading and consequently allows observation of the heart motion throughout the heart

cycle. In combination with ramped flip angles, CSPAMM allows obtaining a constant CNR throughout the cardiac cycle. By applying the tagging preparation in three spatial directions and using a 3D gradient echo sequence for readout, a 3D motion-encoded dataset of the whole heart can be acquired. Together with a 3D HARP evaluation tool, the method enables the 3D quantification and selective viewing of the local myocardial motion pattern under different views and angles throughout the entire cardiac cycle.

A disadvantage of CSPAMM is that it increases the image acquisition time and is prone to slice mis-registration. So during the whole process of CSPAMM, breath-holds are needed. Typical breath-hold techniques pose challenges for achieving all three imaging considerations within clinical acceptable breath-hold duration of 15-20s at end-expiratory breath-hold positions. One approach to reduce the scan time (breath-hold duration) is acquiring two orthogonal line-tagged images with asymmetric k-space sampling within narrow regions of the harmonic peaks rather than a grid-tagged image with isotropic resolution.

Except for CSPAMM, other tagging techniques such as spatial modulation of magnetization (SPAMM), DANTE, sinc-modulated DANTE, radial tags and hybrid SPAMM/DANTE have successfully been applied for the acquisition and quantification of a 2D projection of the underlying 3D myocardial motion.

In data post-processing, although the tag line deformation in cine display can be tracked and analyzed visually, this approach is subjective and limited by image quality. Motion quantification techniques (17) are divided into:

1) Differential optical flow-based methods that track motion by assessment of the temporal and spatial changes of image intensity;

2) Tag segmentation methods based on tracking of tag lines as in Findtags and SPAMMVU analysis;

3) Phase-based analysis methods which are the bases for Harmonic phase (HARP) analysis.

In our research we choose the method of HARP. The HARP method facilitates automated motion tracking of tissue. It is currently the most widely used method for strain quantification because it is highly automated, limits both analysis time and subjective interference. HARP analysis of myocardium on tagged MRI images is 10 times faster than conventional tag analysis and almost as accurate. Further more, subtle changes that occur in myocardium during stress testing or after infarction can be measured with HARP analysis. The HARP calculates for each pixel the spatial phase in the periodic tagging pattern. This technique allows tracking of arbitrary tissue points with the help of their phase information, which remains constant over the whole cardiac cycle. With HARP, a single motion-encoded harmonic peak is isolated using a bandpass

filter decomposing the tagging signal into signal vectors of constant amplitude and spatially varying phase. The filter radius of the HARP bandpass filter is typically chosen to be less than the tagging frequency in order to exclude any residual signal from incomplete subtraction of the signal components arising from T1 relaxation (18). HARP allows for calculation of the deformation directly by calculating the regional spatial frequency of the tagging pattern and comparing it with the under formed frequency (16). The harmonic phase in image-space moves with the underlying tissue and can therefore be used to track material points.

It has been shown that the use of CSPAMM yields significantly better strain results when HARP analysis is used. Although traditionally the HARP method is optimized for high temporal resolution and low spatial resolution, and displacement-encoded imaging with stimulated echoes for low temporal resolution and high spatial resolution, this is not an essential difference intrinsic to the either method. A recent extension of the HARP method, with peak-combination HARP analysis where signals from conjugate harmonic peaks are utilized rather than from a single peak, resulted in yielding improved signal-to-noise ratios (SNRs) in HARP procession. To form a single HARP image, the harmonic phases from conjugate peaks are subtracted, thereby also eliminating phase errors from B_0 inhomogeneities that are additive to the conjugate peaks. It has been shown that such a scheme results in reduced tracking errors and therefore improved accuracy and reproducibility of HARP processing (17).

1.4 β-Blockers

Early in heart failure, drops in cardiac output lead to decreased organ perfusion, a compensatory increase in adrenergic drive, and the subsequent release of neurohormones such as norepinephrine. In turn, norepinephrine in the cardiac adrenergic drive stimulates ventricular contraction and increases vascular resistance, thereby increasing cardiac output and blood pressure. This chronic activation of the adrenergic nervous system leads to several potentially deleterious effects on the heart. Sustained adrenergic activation and norepinephrine release raise cardiac output and heart rate, which then increase myocardial oxygen demand, ischemia, and oxidative stress. As the neurohormonal hypothesis emerged, also a new understanding of the potential role of β-blockers in heart failure appeared. β-blockers are a commonly prescribed class of medications that are known to improve the outcomes of patients with left ventricle (LV) systolic dysfunction. Over the past decades, the position of β-blockers in heart failure (HF) has evolved from contraindication to established treatment. Historically, β-blockers were contraindicated in patients with HF due to their negative inotropic effect. However, as the neurohormonal paradigm of HF was appreciated, there was an increasing interest in the β-

blockers. β-blockers are competitive antagonists at the β-adrenergic receptors, thereby reducing the level of sympathetic nervous system activation. Now β-blockers are considered beneficial in patients with heart failure in terms of reducing hospitalisation, improving left ventricular function, slowing of heart failure progression and increasing life expectancy. Long term treatment with β-blockers has also been shown to reduce the need for cardiac transplantation (19). Using β-blockers as a treatment of HF is established as a part of standard therapy in patients. Clinical trials have shown that β-blockers can reduce mortality of HF and improve quality of life by decreasing sympathetic drive which is chronically increased in HF, and by disturbing and interrupting neurohumoral pathways. It can reduce the mortality of HF by approximately 25% (20). Although β-blockers are established as a part of standard therapy in patients with heart failure, not all β-blockers have shown the same beneficial effects in heart failure patients. In addition, there is variability in responses to β-blockers among patients. β-blocker therapy requires a careful monitoring and slow dose titration to minimize adverse events from the drug (21). Despite careful titration, approximately 25% of patients require discontinuation of therapy due to intolerance to the drug (22).

The rationale for the use of β-adrenergic receptor antagonists in HF patients is based on observations that sympathetic efferent neuronal activity is increased in HF and that this sympathoexcitation has independent prognostic value. There are α and β receptors which have been found in most organs apart from the heart. α-receptors have been found to occur presynaptically at post-ganglionic cardiac neurons. Their function is to control the amount of noradrenaline released after sympathetic stimulation by a feedback mechanism. Most of the myocardial β-receptors are of the β_1-subtype. Just a few are of the β_2-subtype. Sympathetic nervous system activation is prolonged in patients with heart failure. There is a down regulation of β_1-receptors in the failing heart. β_1-receptors are reduced in number and density whereas the number of β_2-receptors remains unchanged. In contrast to the reduction of β_1-receptors, the percentage of β_2-receptors increases from 20% up to 40% (23). β-blockers may provide cardiac protection in HF via a blockade of postsynaptical β-adrenergic receptors on cardiac myocytes. Another mechanism by which β-blockers may be beneficial is through the antagonism of postsynaptical β_2- adrenergic receptors, which facilitate neural norepinephrine release.

The current β-blockers used and approved for heart failure can be divided into two major categories: second-generation selective including Metoprolol, Esmolol and third-generation non-selective β-blockers such as Propranolol or Timolol. The second-generation β-blockers are designed to be preferentially β_1-receptor selective. The selective β-blockers are normally indicated for patients in whom β_2-receptor antagonism might be associated with an increased risk

of adverse effects. Such patients include those with asthma or diabetes, or patients with peripheral vascular disease or Raynaud's disease (24). But when these agents are used at high doses, they will lose their β-receptor-selectivity properties and their potential effect may be altered (25). Besides this, several of the second-generation β-blockers have been shown to have additional properties, including anti-oxidant and vasodilator effects. The third-generation β-blockers are non-selective agents that attempt to counteract the adrenergic system at multiple sites. Some agents exist β-1, β-2 and α-1 blockade. They have also been proven antioxidant, antiapoptotic and of vasodilatory and myocyte energy utilization effects. The nonselective β-blockers cause a significant reduction in cardiac and systemic norepinephrine spillover, an effect that was not observed with the second-generation selective β_1- blockers.

In the neuroendocrine system, β-blockers play an important role. Activation of β_1-adrenoceptors in the kidney leads to release of renin, which stimulates angiotensin II consecutively. Angiotensin II represents a potent vasoconstrictor which increases vascular peripheral resistance. It also leads to renal vasoconstriction and thereby to the release of aldosteron. Therefore it leads to salt and water retention. Catecholamines as well as angiotensin II have additional direct toxic effects on cardiomyocytes. β-blockers can interrupt these neurohumoral activation pathways in order to improve the myocardial function and systemic circulation.

The hemodynamic effect of β-blockers can be considered from acute and chronic changes. β-blockers act as negative inotropic and negative chronotropic agents because of their reduction of cardiac index in the short term. But reducing the heart rate means prolonging diastole. According to this, β-blockers can increase coronary perfusion time. A lower heart rate is also associated with lower myocardial oxygen consumption and further reduction of myocardiac ischaemia. Some researchers found that the patients with dilative and ischaemic cardiomyopathy demonstrated that chronic administration of β-blockers leads to a constant decreased heart rate, whereas blood-pressure remains largely unchanged. There was no negative effect on cardiac index, sometimes cardiac index was even increased. Except for this, β-blockers on the myocardium can also reduce arrythmias, prevent coronary plaque ruptures by modifying the atherosclerotic process even when no effect on platelet aggregation could be demonstrated.

As can be seen, the future of β-blocker therapy may need to focus on the development of harnessing these additional benefits and providing a more ‘balanced’ blunting of the adrenergic system. After all, using the β-blockers at the wrong time in an inadequate dose can worsen clinical symptoms. In the meantime, we will need to optimize our current range of drugs through investigations into the pharmacogenetics, pharmacokinetics and pharmacodynamics of β-blockers.

2 Hypothesis

The architecture of the heart is complex. The typical theory of cardiodynamics by Frank has demonstrated that most of the myocytes are aligned more or less in the tangential plane to the epicardial surface. The prevailing tangential myocytes are relative to the thickness of the ventricular walls, is responsible for overall constriction of the ventricular cavity. The oblique myocytes can engender the auxotonic forces to provide balance for the entirety of the ventricular wall.

To our knowledge, the capacity of drugs, such as barbiturates, to depress contractile forces depending on the afterload exerted on the myocytes has attracted little attention. If we are to understand their therapeutic actions, we must first appreciate the way the myocytes are arranged within the ventricular walls. In this respect the amount and the slope of afterload of an individual myocyte are determined not only by the global haemodynamic resistance of the ventricular outflow, but are also the consequence of the geometrical alignment of the individual myocytes within the ventricular myocardial mesh.

Negative inotropic medication induced a highly significant drop in the auxotonic force. This fall is appreciably less dramatic in the aggregated myocytes parallel to the surface, these aggregated generating the unloading type of tension. Some researchers have found that the population of obliquely orientated myocytes is more sensitive to the negative inotropic action of barbiturates than the myocytes which are aggregated with their long axes tangential to the ventricular walls. Also β-blockers attenuates, instantly and in more efficient fashion, the forces relative to the thickness of the ventricular walls which is produced by the oblique myocytes, as opposed to the constrictive forces provided by tangentially aggregated myocytes. In clinics, treatment with an optimal dose of β-blocker has been shown to give the greatest increase in survival.

On this basis, we postulate that β-blocker, at low doses, exert an instantaneous selective action, which constrains the forces engendered by those myocytes which are aggregated with their long axes oblique relative to the short axis of the ventricular wall. These obliquely aggregated myocytes, as we know, are more sensitive to the depressant action of β-blockers than the prevailing tangentially aggregated myocytes engendering the constrictive activity. If so, the effect of oblique myocytes contraction will be attenuated by low doses of Esmolol which is a short acting β_1-blocker. And with these low doses of β-blocker the attenuation of tangential myocytes contraction will not be severe. That means with less forces provided by oblique myocytes, the tangential myocytes will perform more actively than without blocking oblique aggregates. So from the design of our research, we test the results including the time to maximum contraction, maximum contractive extent, slope (speed to maximum contraction) and

myocardial work (AUC) in circumferential, radial, longitudinal shortening and rotation. If the hypothesis is successful, the maximum contractive extent of low doses will be stronger than of higher doses of Esmolol. The time to maximum contraction will also be shorter than on higher doses. The slope and AUC will also be strengthened. So we expect the results will attend not only in circumference shortening, but also in radial, longitudinal shortening and rotation according to our hypothesis.

3 Material and Methods

3.1 Study Population

We included 13 healthy volunteers with a median age of 36 years (age range from 29 to 41 years). The volunteers were predominantly white, and there was a nearly even distribution of men and women (6 male, 7 female). Before being involved in this study, all participants gave their written consent to be examined. The volunteers' past disease and medical history as well as current health status were explored for adverse events prohibiting the MRI procedure or β-blockers before conducting the MRI. These individuals had no clinical history of cardiovascular disease, diabetes mellitus, or potential cardiac symptoms such as chest pain or dyspnea. This research was approved by Deutsches Herzzentrum Berlin and Charité Medicine University, and was carried out in accordance with institutional guidelines.

3.2 Volunteers Preparation

Before conducting the MRI, every volunteer has a venipuncture in his basilic vein with a three-way stop cock allowing the simultaneous administration of physiological saline and the β-blocker Esmolol. The Esmolol dose was calculated by the weight of every volunteer. Also during conduction of the MRI, the basic vital signs (5-point-electrocardiogram [ECG], non-invasive blood pressure [BP], peripheral oxygen saturation [SpO_2]) were monitored continuously and every 3min respectively. MRI tagging image was performed with the volunteers in the supine position.

3.3 MRI Sequence Parameters

The MRI machine which we used to acquire the tagging data was a 3.0 Tesla (Achieva, Philips Medical Systems, Best, The Netherlands).

3D Tagging acquisition parameters were set as follow:

1) Temporal Resolution (TR) 7.0 ms; 2) Echo Time (TE) 3.2 ms; 3) Flip Angle of 19-25°; 4) Turbo Factor (TF) 28; 5) Number of profiles per Echo-planar Imaging (EPI) segment=7; 6)

TFEPI 42 slices; 7) 3 staple of slices; 8) Slice thickness7.0/0.0mm; 9) Field-of-view (FOV) =108*108*108mm^3; 10) Matrix size=28*14*16; 11) Phases=24; 12) NSA=2.

The utilization of a patch of Philips Achieva system is necessary for acquisition of CSPAMM. Within the exam card of the 3D tagging sequence the spoiler factor which sets the duration of spoiler gradients in the tagging sequence keep in the default of 4 (range 1-20). The rectangular field of view (RFOV) is set to 95% (range 25-100%). This selects the field of view (FOV) percentage of the total FOV. And flip angle optimization for TFEPI scans should be chosen (18).

3.4 CSPAMM (Complementary Spatial Modulation of Magnetization) Technique

A disadvantage of CSPAMM is that it increases the image acquisition time. For our research, a fast method for acquiring 3D CSPAMM data is proposed that allows to measure myocardial deformation of the entire left ventricle in three short breath-holds. The acceleration is achieved by splitting the acquisition into three orthogonally motion-encoded 3D measurements and by applying a localized tagging preparation in combination with a hybrid multi-shot, segmented echo-planar imaging (EPI) sequence (26). CSPAMM tagging preparation generates a 3D tagging grid on the myocardium. Two 90 ° block pulses, interspersed by a dephasing gradient, produce a sinusoidal modulation of z-magnetization and thus a line shaped tag pattern (27). The tagging preparation is applied at end-diastole, after the detection of the R-wave of the ECG. As normal, the duration of the MRI tagging preparation is 12 ms.

3.5 MRI Tagging Protocol

This study was designed as an open-labeled, interventional, unblended, non-randomized study. Our MRI tagging protocol can be divided into two stages (14):

1) Producing a spatially modulated pattern of saturated magnetization in the heart using a combination of radio-frequency (RF) and gradient pulses;

2) Imaging the deformation of the pattern using virtually any desired ECG-gated pulse sequence.

Throughout the whole procedure, the basic vital signs (ECG, BP, SpO_2) are monitored every 3min. After baseline acquisitions, we inject Esmolol doses in following steps, with MRI sequences starting 4 min after Esmolol dose change:

1) Esmolol (Brevibloc^{TM}): Dose-0μg/kg/min intravenous injection
   MRI: phase contrast flow across aorta, 3D Tagging
2) Esmolol (Brevibloc^{TM}): Dose-5μg/kg/min intravenous injection
   MRI: phase contrast flow across aorta, 3D Tagging
3) Esmolol (Brevibloc^{TM}): Dose-10μg/kg/min intravenous injection

MRI: phase contrast flow across aorta, 3D Tagging

4) Esmolol (Brevibloc™): Dose-25µg/kg/min intravenous injection

MRI: phase contrast flow across aorta, 3D Tagging

5) Esmolol (Brevibloc™): Dose-50µg/kg/min intravenous injection

MRI: phase contrast flow across aorta, 3D Tagging

6) Esmolol (Brevibloc™): Dose-100µg/kg/min intravenous injection

MRI: phase contrast flow across aorta, 3D Tagging

7) Esmolol (Brevibloc™): Dose-150µg/kg/min intravenous injection

MRI: phase contrast flow across aorta, 3D Tagging

Each dose of Esmolol was successively injected over a period of approximately 12-13 min with an initial interval of 4min before starting MRI scanning. MRI investigation at different doses comprised a complete set of short and long axis views of the left ventricle, a set of 3D Tagging data with a grid inter space of 7mm and acquisition of phase contrast flow measurements in the ascending aorta. The image acquisition of the scan actually is split into several breath-holds due to the lengthy measurement. The optimal end-expiration breath-hold position and duration within a clinically acceptable duration of 15-20s are chosen by the volunteer in a reference measurement, completed before the main data collection (27). During the breath holds, typically one inspiration cycle is performed. After conductance of the tagging sequence at each dose step, the shift parameters are displayed and listed for post processing.

3.6 MRI Tagging Image Analysis

For short axis the analysis of circumferential and radial shortening as well as rotation, we divided the whole heart of every volunteer into 4 representative slices from apex to base (1.apex, 2.mid-apex, 3.mid-base, 4.base) within 24 phases of a whole cardiac cycle. Every slice is divided into 6 sectors (S1-S6). S1 is defined in the septal wall, subsequent 60°-sectors are numbered consecutively in clockwise direction as viewed from the apex. Post procession started with analysis the REC files on the MRI console in order to reconstruct the images. Analysis of longitudinal axis was the same except that there only one sector on one midcaval slice existed. Mid-wall contours consisting of multiple landmark points were drawn thus tagging on different short axis and on the longitudinal axis slice in the end-diastolic images. A time frame with good blood-myocardium contrast was chosen for contour definition. The contours were subsequently HARP-tracked through 24 frames throughout the cardiac cycle and located on successive images. Data post-processing of MRI tagging on short axis including circumferential, radial shortening as well as rotation, was performed by using software 3D TagTrack (version 1.5.2, GyroTools,

Zurich, Switzerland). And MRI Tagging on longitudinal shortening was performed by using software 2D TagTrack (version1.5.2, GyroTools, Zurich, Switzerland). TagTrack can conduct different kinds of data, such as 2-line-tagging, 3-line-tagging, grid tagging or CSPAMM and SPAMM. Generally CSPAMM gives superior results compared to SPAMM because of better differentiation of tagging frequencies in k-space. For Cartesian acquisitions line-tagging is better than grid-tagging because of the better performance of the peak combination method. But grid tagging makes more sense for spiral acquisition. Before tagging with the software, we had to prepare the images including:

1) Suppression of background intensity variation due to non-uniform RF fields;

2) Suppression of thermal noise;

3) Normalization of image intensities (14).

There are four menus (Dataset, Contours, Statistics, Options) on the control panel of the software TagTrack. The dataset menu displays general information of the current application data. A gallery viewer allows a quick survey of the data.

In the options panel, one can set parameters: Track Algorithm, Peak Selection, Cardiac Wall Segmentation, Cardiac Wall Sectors, DataSet, Filter Width and Filter Position. We set the Reference Phase to 24 in which the heart is in end-diastolic state and the error tolerance is set to 0.1. Others are set automatically (Fig.3.6.1).

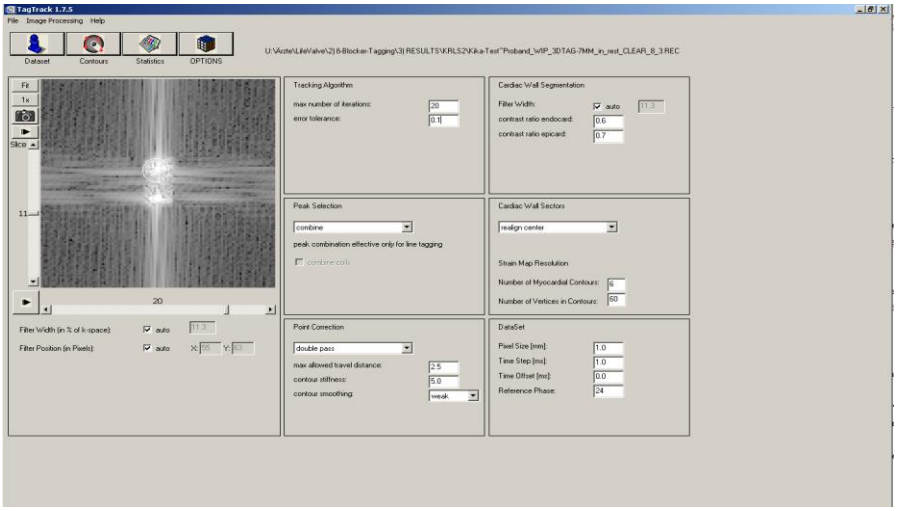

Fig.3.6.1 Menus of software TagTrack

The contour menu features the main viewer and the contour creation as well as editing tools. In this menu we can tag myocardium and track contours. The time and slice sliders allow scrolling through all the images of the data set. The statistics page features plots of statistical values derived from valid tracks. Tracks validated from contours are shown in the contour menu upon each entry of the statistics menu.

After the setting, we began tagging on myocardial MRI images in the contours menu. The contour tracking occurs in two steps. First, all contours are tracked using the conventional HARP method. Second, the peak-combined HARP image is used to re-adjust each landmark point to its corresponding phase.

We tag the images according to following protocol (Fig.3.6.2-3):

1) Adjust the direction of the image to allow for better tagging

2) Choose a better slice in which the heart can stay in the most diastolic situation

3) Set Name, Colour, Visible, and set Type as midline

4) Tag the image in the middle of the myocardial

5) After tagging the image, adjust the tagging point to make sure it is in the middle

6) Interpolate the contour

7) Track the contours forward or backward (24 Phases of the whole cardiac cycle) of the selected contour

Normally after these protocols, each slice image of the cardiac cycle obtains a contour within all phases of the short axis or the long axis.

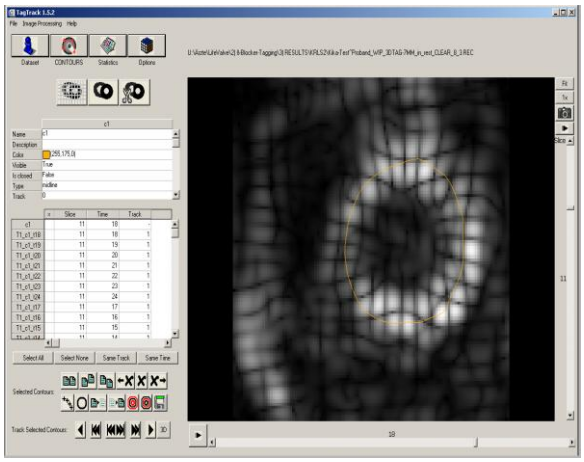

Fig.3.6.2

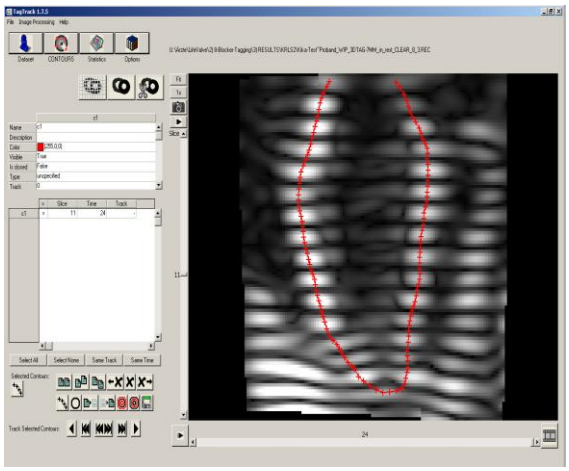

Fig.3.6.3

Fig.3.6.2 Myocardial tagging on a short axis image over 24 phases

Fig.3.6.3 Myocardial tagging on a long axis image over 24 phases

After tagging the images, the analysis can be viewed in the statistics menu. For 3D TagTrack software one can save the results directly for the separate 6 sectors (Fig.3.6.4). But for 2D TagTrack software (tagging longitudinal shortening) we had to set 1 sector only, because division of the long axis in sectors is not a standard model.

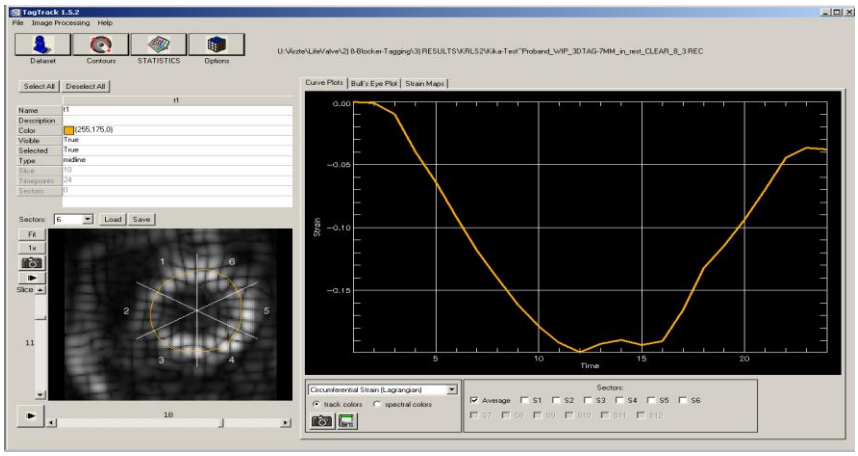

Fig.3.6.4 Statistic of Myocardial Tagging on circumferential shortening

Every quantitative result of the myocardial deformation by Tagging was saved as a .txt file in the form of values for circumferential shortening, radial shortening, rotation, longitudinal shortening and then imported into excel in order to analyze the data. To do this the .txt file is opened with Excel. Then the relevant numeric data is marked and all decimal numbers containing a decimal point instead of a comma are converted. As normal, the numbers are separated by a space or semicolon. So the values are converted into columns of Excel in order to create a table of values. Also the additional information such as the name of the volunteer, information on slice, sector and heart phase has to be saved to ensure that each value can be properly allocated to a region of the heart.

3.7 Statistics

The extracted myocardial motion parameters of the volunteers for circumferential, radial, longitudinal shortening and rotation on different cardiac levels and in multiple sectors were plotted as medium with quartile width and as mean with standard deviation over time using box-plots and diamond plots respectively. We used the Wilcoxon Test (IBM SPSS Statistics 19) and Analyse-it V2.22 for data analysis.

4 Results

The tagging measurements were successfully accomplished in all 13 volunteers. Hemodynamic parameters and cardiac rhythm remained stable during the MRI tagging image acquisition. Esmolol was well tolerated by all volunteers. Also the breath-hold duration was well tolerated by all subjects. The time of the investigation added up to a median of 1.7 hours including preparation and final data processing to generate the REC files for 3D TagTrack and 2D TagTrack. Selected time-frames (phases) are shown in Fig.4 for a single slice including

circumferential shortening and longitudinal shortening. At end-systole, tagline deformation due to myocardial contraction and rotation (left figure in Fig.4.a) as well as a decreased tag distance due to longitudinal shortening of the left ventricle (left figure in Fig.4.b) can be observed.

(a)

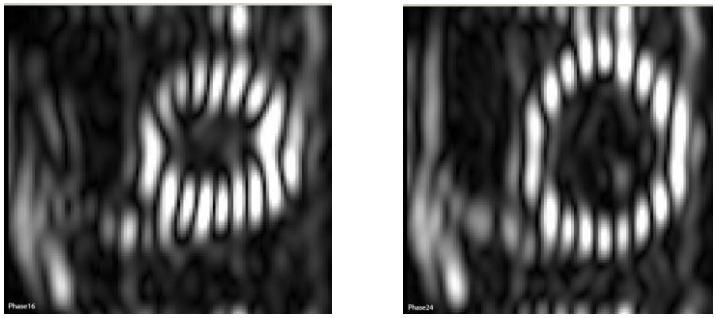

(b)

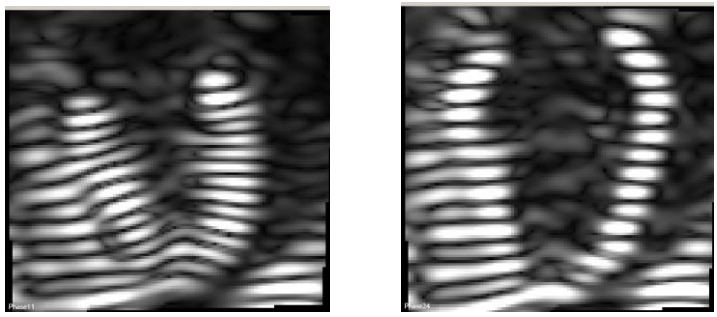

Fig.4 Exemplary slices of tagged myocardium of a volunteer for circumferential shortening and longitudinal shortening. (a) phase 16: end-systole heart, phase 24: end-diastole heart; (b) phase 11: end-systole heart, phase 24: end-diastole heart

4.1 Curve analysis

The values for circumferential, radial and longitudinal shortening as well as for rotation were displayed as curves with time line in form of heart phases within one heart cycle on the abscissa and the amplitude of the curve on the ordinate.

We analysed the results from four areas including circumferential shortening, radial shortening, longitudinal shortening and rotation to detect different doses of Esmolol effect on the different shortening patterns (4.1.a). In every area we defined four kinds of values (maximum of the curve, area under the curve (AUC), time to maximum and upslope of every curve) (Fig.4.1.b).

The maximum movement of myocardium (MAX) is on behalf of the myocardial contraction force which is represented by the amplitude (%) from curve vertex to starting point.

Time to maximum amplitude (Tmax) of myocardial contraction reflects the systolic duration to reach the maximum contraction. It can show the myocardial systolic efficiency.

The area under the curve (AUC) is a calculation of ventricular work and is achieved by summing up all values (%) of the curve within all heart phases (one heart cycle).

The upslope of every curve stands for ventricular contraction speed or contraction rate. It is calculated by dividing the curve maximum by the time to maximum.

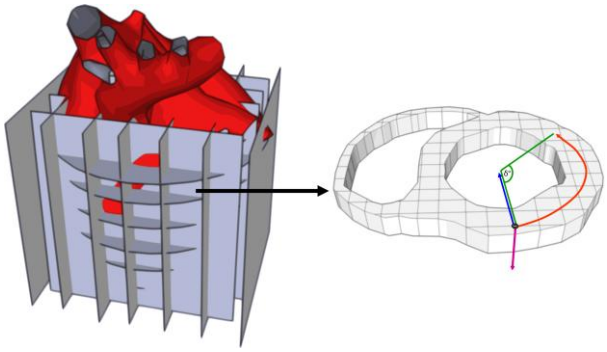

Fig.4.1.a

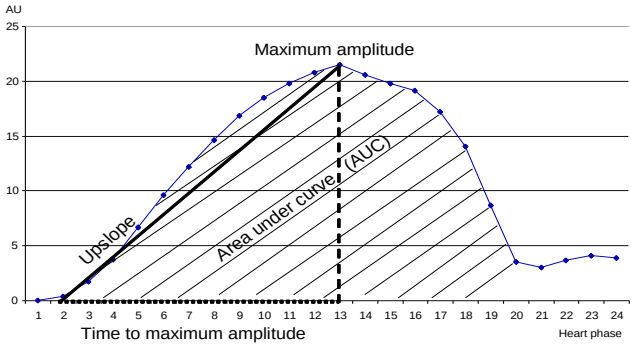

Fig.4.1.b

Fig.4.1.a The images are post-processed slicewise using a tracking program resulting in a curve throughout the 24 heart phases for circumferential shortening (red line), radial shortening (blue line), longitudinal shortening (pink line) and rotation for each slice (green angle)

Fig.4.1.b For each curve the Maximum amplitude of the myocardium, the Time to maximum, AUC and Upslope are obtained and analyzed

Curve analysis for effect on myocardium with different doses of Esmolol

We divided the heart of every volunteer into 8-12 slices from apex to bottom of the heart depending on size and image quality. 4 representative slices 1) apex, 2) apical mid, 3) mid-to-base, 4) basis were chosen. Every slice was divided into 6 sectors (S1-S6). We tagged every sector within 24 phases of a whole cardiac cycle. For the obtained CS, RS, LS and ROT values of the healthy volunteers, average values over all vectors were calculated. Then we calculated the average value of 4 slices and took it as one volunteer's value. Last we calculated 13 volunteers' averages on different β-blocker doses as the values. Every area which we detected including circumferential, radial, longitudinal shortening and rotation was made in the same way. The results can be seen as follows:

4.1.1 Circumferential Shortening

This is a typical curve to show that different doses of Esmolol have different effect on the myocardium. We could see from (Fig.4.1.1.a-c): The dose (0 µg/kg/min, basic curve) is displayed with no influence of β-blocker medication (Esmolol). When the doses of Esmolol are added from 5 to 25 µg/kg/min, all the three curves move to the left (Fig.4.1.1.a). It is visible that the maximums of the curves are higher than the basic curve (0 µg/kg/min). At the same time,

moving of the maximum to the left shows that the time of heart contraction is shorter than the basic curve.

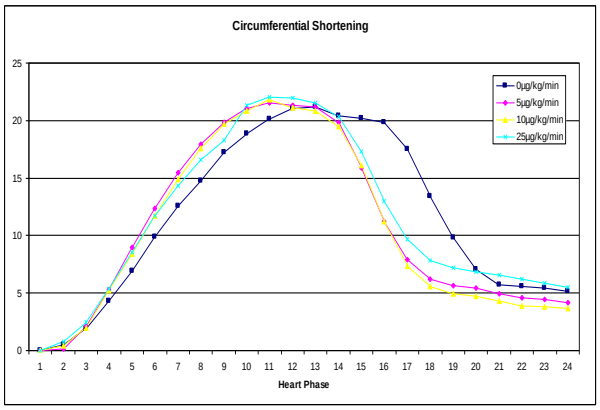

Fig.4.1.1.a

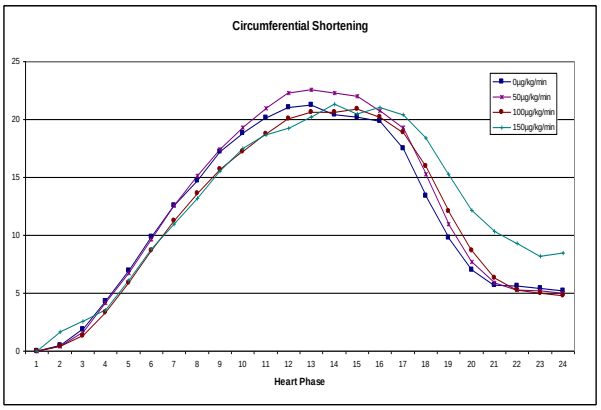

Fig.4.1.1.b

Fig.4.1.1.a With lower doses of β-blocker (Esmolol), the curves move left in contrast to the basic curve (0 µg/kg/min). The maximum movement of the myocardial is more obvious and the time to the maximum movement is shorter.

Fig.4.1.1.b As the doses of Esmolol are increased, the curves shift to right in contrast to the basic curve. The time to maximum movement is longer than the dose 0 µg/kg/min.

More curves are generated with increasing doses of Esmolol. When we injected Esmolol at 50 µg/kg/min, the left shift still exists and the maximum of its curve is also higher than the basic curve. But obviously from 100 µg/kg/min injected, the curves provoke a right shift during later heart phases (Fig.4.1.1.b). The maximum of the curves was not changed significantly. But the time to maximum apex became longer than the basic curve. That indicates that the time of systole prolonged. It can prompt that the efficiency of the heart contraction decreases. Fig.4.1.1.c shows the curves with all doses from 0 to 150 µg/kg/min.

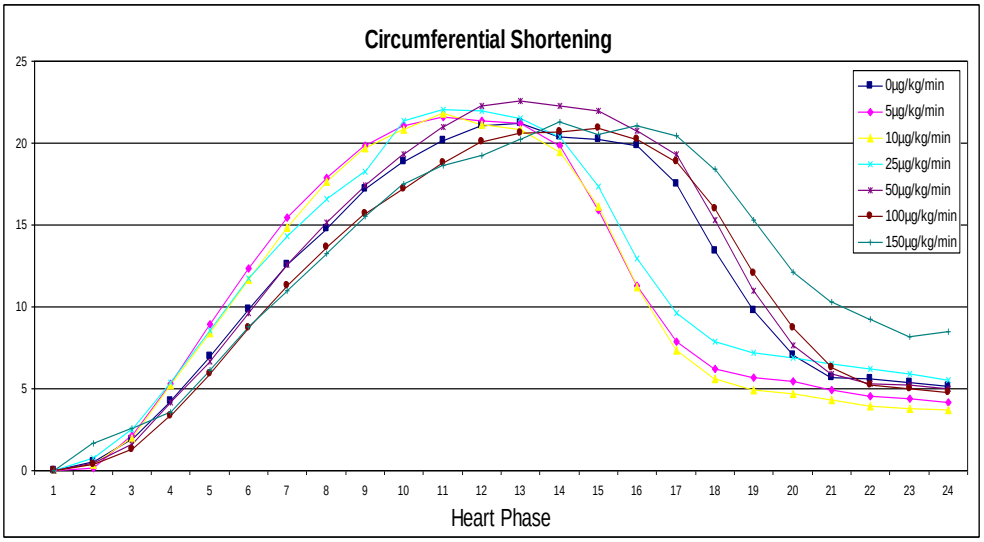

Fig.4.1.1.c Typical curves of circumferential shortening derive from 3D myocardial tagging data on average of all slices with different doses of Esmolol.

4.1.2 Radial Shortening

The curves on radial shortening with different doses of β-blocker (Esmolol) are quite similar with the curves on circumferential shortening (Fig.4.1.2). With lower doses (from 5 to 25 μg/kg/min) injection, the curves shift left. The maximum apexes of the curves are higher than the basic curve (0 μg/kg/min). So the radial shortening reflecting contraction is stronger than without β-blocker. The time to maximum shortening is shorter than the in basic curve. That means faster contraction and relaxation during the cardiac cycle can be observed from three contours with lower doses 5, 10, 25 μg/kg/min. As a larger dose 50 μg/kg/min is injected, the maximum also exceeds the maximum of the basic curve. But the time to maximum of the curve is getting longer. When Esmolol is injected from 100 to 150 μg/kg/min, the curves move right and the amplitude of the curves decreases lower than the basic curve. The time to maximum contraction becomes longer as well as the contraction force becomes less according to the maximum apexes of the curves. Although at the dose of 50 μg/kg/min the maximum of the curve is higher than at the dose 0 μg/kg/min, the time of maximum contraction becomes longer.

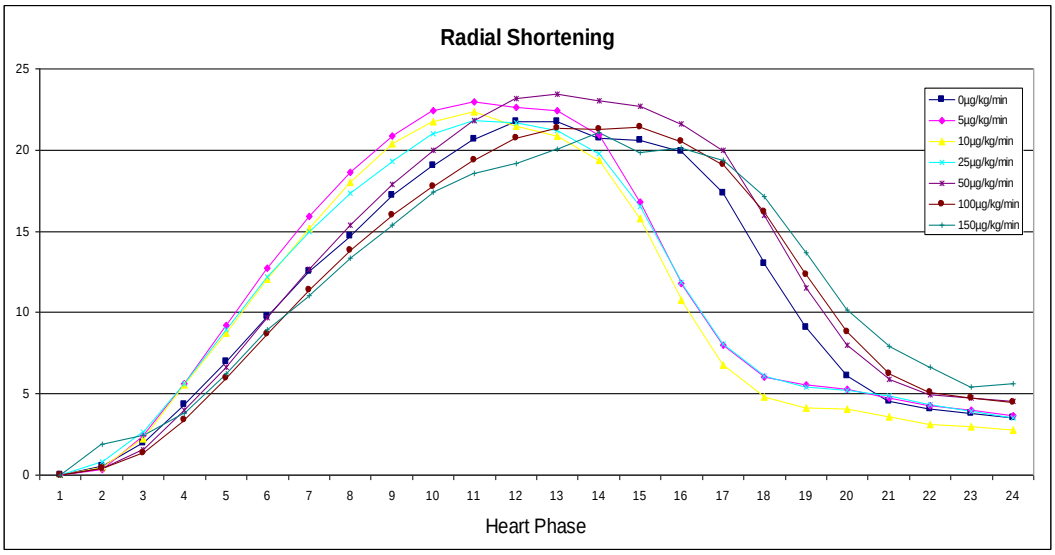

Fig.4.1.2 The movement of myocardium in radial shortening with different doses of Esmolol

4.1.3 Rotation

The myocardium moves circumferentially and longitudinally during the systolic phase of each cardiac cycle which is usually referred to as rotation. The contracting myocardium exerts the rotation to eject blood from the left ventricle. The twisting motion of the heart comes from potential elastic energy by straining the extracellular matrix which is released during early

diastole and therefore probably contributes to early diastolic suction. This rotation is counter-clockwise seen from the apex and clockwise from basis around the ventricular long axis. For the heart rotation with influence of different doses of Esmolol, we can also see similar changes as in circumferential and radial shortening (Fig.4.1.3). The rotation of the heart is much more evident with the doses of 5 to 25 µg/kg/min because of the curves turning left. The time to maximum apexes of the curves is shorter than the dose 0 µg/kg/min. From the results in Fig. 4.1.3, we can prompt that during systole the heart contracts faster and diastole is much shorter with high doses of Esmolol (from 5 to 25 µg/kg/min). For the three higher doses (from 50 to 150 µg/kg/min), the time of systole may be equal or longer compared to the basic curve. But the amplitudes of the curves show lower values and the diastole is shorter than with no β-blocker injected. So with higher doses of Esmolol, the rotation of the heart becomes less pronounced.

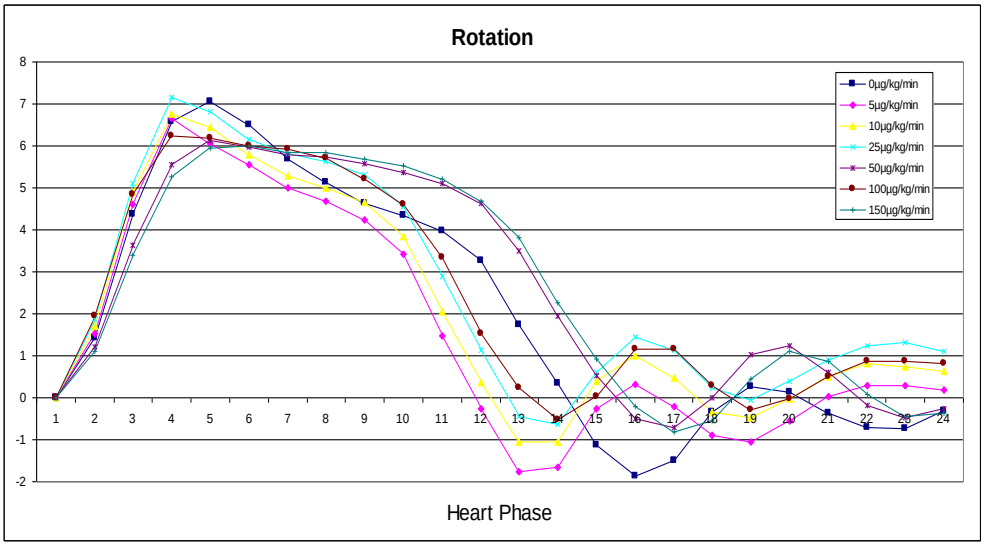

Fig.4.1.3 The rotation of the heart with different doses of Esmolol.

4.1.4 Longitudinal Shortening

Myocardial movement in longitudinal shortening is another way to detect β-blocker influence. The contraction of myocardium does not only act in circumference and radiance but also in the long axis. Fig.4.1.4 shows us that with different doses of Esmolol from 5 to 150 µg/kg/min, the amplitudes between the starting point and the minimum of the curves become smaller and smaller. It can be explained that the contraction of the heart in the long axis gets weaker. But for the lower doses 5, 10, 25 µg/kg/min the time to the minimum of the curves becomes shorter than for the dose 0µg/kg/min. So the time for contraction is shorter. And for the other three doses (from 50 to 150 µg/kg/min), their minimum apexes of the curves shift right. The time to maximum movement becomes longer than in the basic curve (0 µg/kg/min).

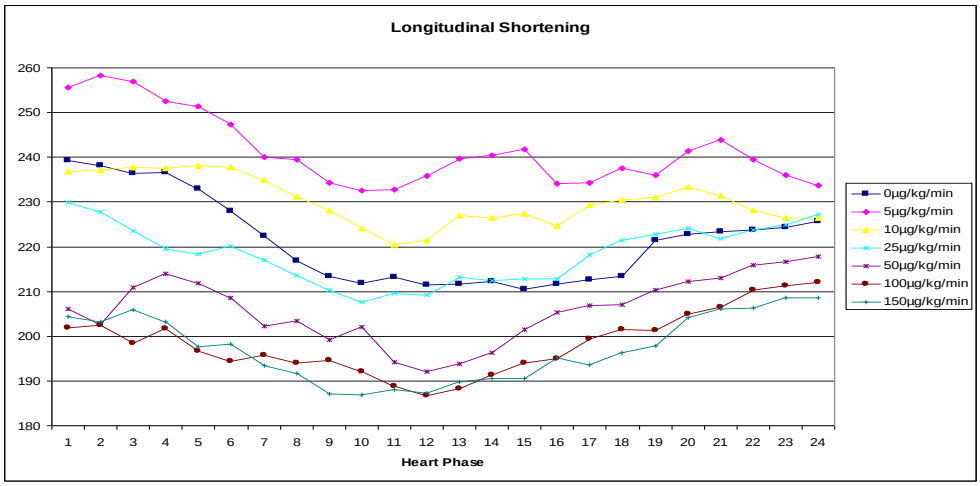

Fig.4.1.4 The curves of longitudinal shortening with different doses of Esmolol become flatter when the doses increase higher.

4.2 Statistical analysis of the effect of different doses of β-blocker on myocardium

Not only did we perform visual analyzing of the typical curves of the volunteers, but also we calculated all the volunteers' average data to detect the different effects with different doses of β-blocker (Esmolol) by statistical test. The analysis takes into account four categories consisting of circumferential shortening, radial shortening, rotation and longitudinal shortening. For every category we also took four active characteristics such as maximum of myocardial shortening (MAX), area under the curve (AUC), time to myocardial maximum movement (Tmax) and upslope (the speed of myocardium contraction). From these four characteristics we could analyze the contraction force, systolic duration, contraction speed and ventricular work. As reported before, we divided the heart of every volunteer into 4 slices from apex to base of the heart within 24 phases of a whole cardiac cycle. Every slice was divided into 6 sectors (S1-S6). Firstly we took the average of 6 sectors of each slice as one slice average value within 24 phases during one cycle. Then we took the average of the 4 different slice averages values as one volunteer's value. We calculate the values for all the doses. Then we analyzed the difference of all the average values using the softwares Analyse-it V2.22 and IBM SPSS Statistics.

4.2.1 Circumferential Shortening (CS)

4.2.1.1 Maximum

Fig.4.2.1.1 shows us the different contraction maxima of circumferential shortening over one cardiac cycle with different doses of Esmolol. In the figure, the box charts show the median and 95% confidence interval of all the values within one dose during one heart cycle. The diamond charts show the mean and 95% confidence interval of all the values within one dose. We can see

from the figure that from dose 5 to 25 μg/kg/min, the medians and means are higher than for the dose 0 μg/kg/min. But from dose 50 μg/kg/min the line drops. We can deduce that the doses 5, 10, 25 μg/kg/min give much more positive effect on the movement of the myocardium than doses 50, 100, 150 μg/kg/min from the changes of the curve.

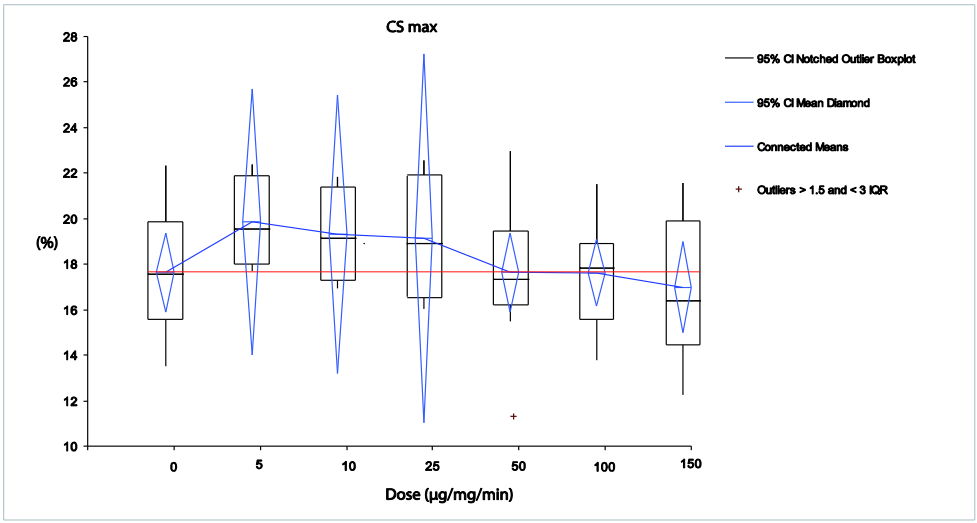

Fig.4.2.1.1 The maximum movement of myocardium in Circumferential Shortening (CS) with different doses of Esmolol; the red line is the mean value of myocardial maximum movement without Esmolol.

4.2.1.2 Area under the Curve (AUC)

The area under the curve means the work of the myocardium during the cardiac cycle. From Fig.4.2.1.2, we can see that AUC also goes up and then drops off. In three lower doses 5, 10, 25 μg/kg/min the medians and means are higher than the dose 0 μg/kg/min (basic dose). From dose 50 μg/kg/min, the values are lower than the basic dose. So it can show that within the doses 5, 10, 25 μg/kg/min the conferential shortening of myocardium is much stronger.

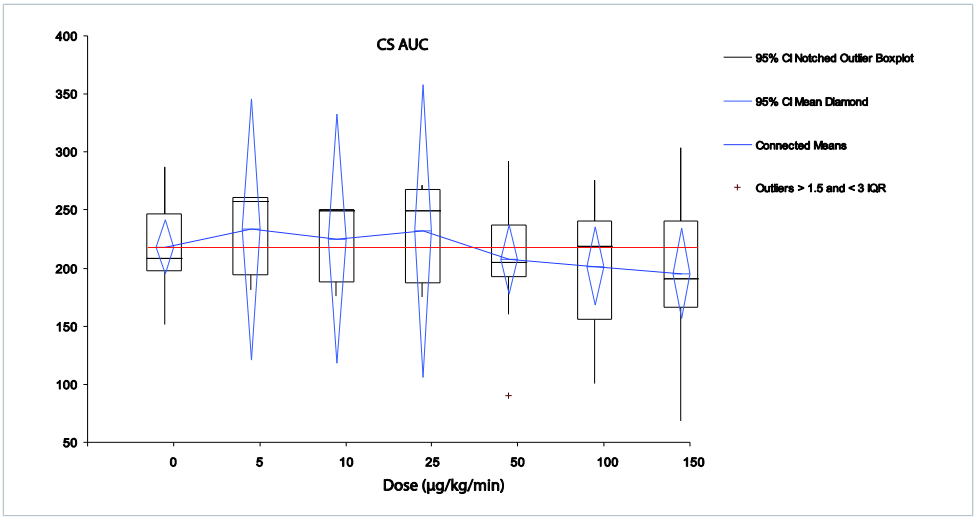

Fig.4.2.1.2 The area under the curve (AUC) in Circumferential Shortening (CS) with different doses of Esmolol; the red line is the mean value of myocardial maximum movement without Esmolol.

4.2.1.3 Time to Maximum

The time to maximum reflects the systolic duration to reach the maximum contraction. In this graph (Fig.4.2.1.3), the time to maximum in circumferential shortening becomes shorter when Esmolol at 5 µg/kg/min is injected. When we injected at 10 µg/kg/min, the time to maximum contraction became shortest. From dose 25 µg/kg/min within all doses of Esmolol injected into volunteers, the time is shorter than at the basic dose (0 µg/kg/min). Especially for the three doses 5, 10, 25 µg/kg/min, the time is much shorter than in higher doses. We can conclude that the time of myocardial contraction in general becomes shorter under the influence of Esmolol. The lower doses (5, 10, 25 µg/kg/min) prove to be of more effect.

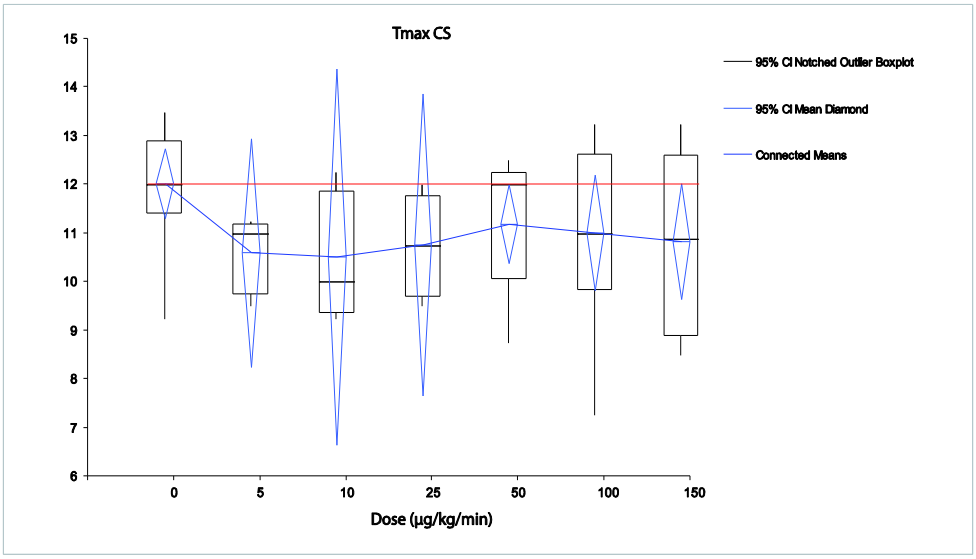

Fig.4.2.1.3 The time of maximum movement in Circumferential Shortening (CS) with different doses of Esmolol; the red line is the mean value of myocardial maximum movement without Esmolol.

4.2.1.4 Upslope

The upslope of the curve stands for myocardium contraction speed or contraction rate. It is calculated by dividing the curves' maximum amplitude by the time to maximum. From Fig.4.2.1.4, we can see the upslope go sharply up from dose 5 µg/kg/min followed by a decent beginning at 25 µg/kg/min. And then the line curves down. We can see that the three doses 5, 10, 25 µg/kg/min are almost at the same level which is significantly higher than that of the other three doses 50, 100, 150 µg/kg/min. In general the upslope of all the doses using Esmolol is higher than without Esmolol. So with the effect of Esmolol, the myocardium contracts faster than without β-blocker injected. At lower doses the effect is more obvious than the other three doses. The trend on medians of different doses Esmolol changes similar to the means.

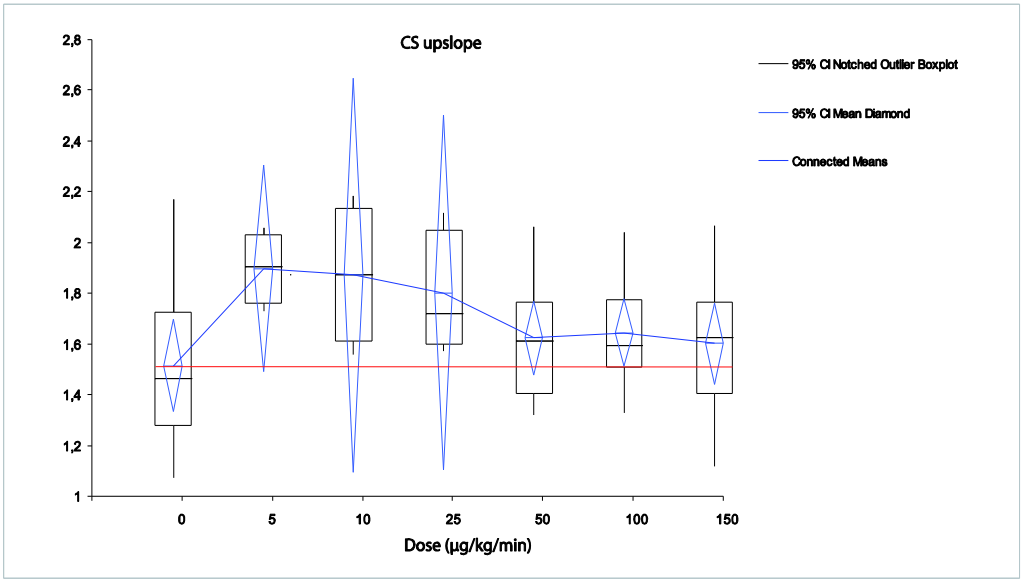

Fig.4.2.1.4 The upslope of Circumferential Shortening (CS) with different doses of Esmolol; the red line is the mean value of myocardial maximum movement without Esmolol.

In the four analysis (CS max, CS AUC, CS time, CS upslope) the three doses 5, 10, 25 µg/kg/min show a more pronounced effect than the higher doses. So we state from radial shortening, longitudinal shortening and rotation that the lower doses of the β-blocker Esmolol have more effect on the myocardium.

4.2.2 Radial Shortening

4.2.2.1 Maximum

When the heart contracts, the myocardium moves not only in the circumference but also in radial and longitudinal direction. According Fig.4.2.2.1, we could see that when given 5 µg/kg/min of Esmolol, the RS became intensely stronger. With increasing doses, the curve of RS went down little by little. But the medians and means remained still higher than at 0 µg/kg/min. When we administered the drug at doses of 50 and 100 µg/kg/min, medians and means were quite near to the basic dose. With dose 150 µg/kg/min, the median and mean were lower than with a dose of 0 µg/kg/min.

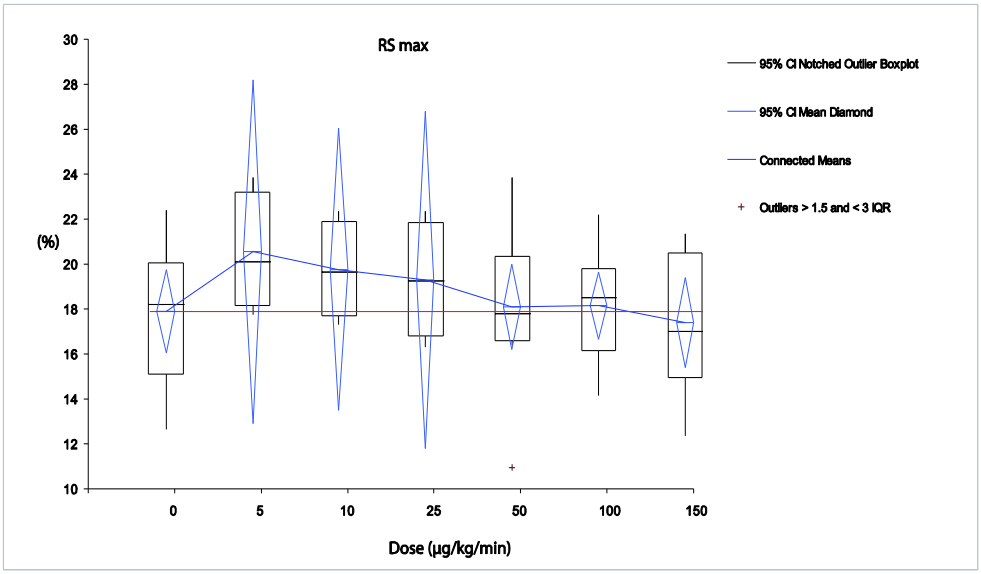

Fig.4.2.2.1 The maximum movement of myocardium in Radial Shortening (RS) with different doses of Esmolol; the red line indicates the mean value of myocardial maximum movement without Esmolol.

4.2.2.2 Area under the Curve (AUC)

Fig.4.2.2.2 shows the changes in Radial Shortening AUC during Esmolol administration. Means go up from the dose of 5 µg/kg/min during the three low doses the curve keeps almost stable and higher than without Esmolol. But from dose 50 µg/kg/min, the curve declines and means get lower than without Esmolol.

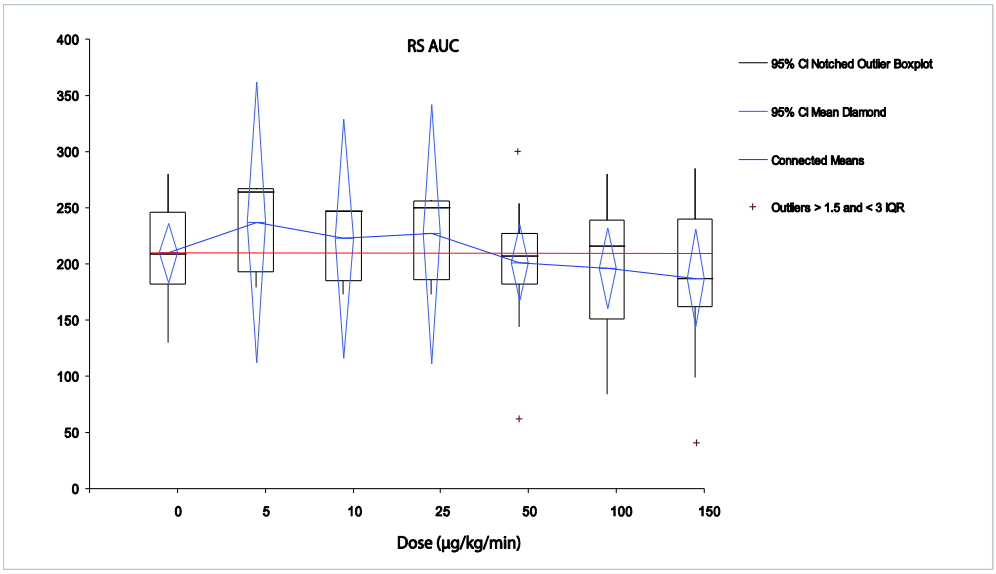

Fig.4.2.2.2 The area under the curve (AUC) in Radial Shortening (RS) with different doses of Esmolol; the red line is the mean value of myocardial maximum movement without Esmolol.

4.2.2.3 Time to Maximum

The result (Fig.4.2.2.3) of time to maximum movement (Tmax) in radial shortening is very similar with the results of circumferential shortening. After using Esmolol, the time of myocardial contraction in radial direction is shorter than without Esmolol. From dose 5 µg/kg/min the time becomes vastly shorter. And with a dose of 10 µg/kg/min, the time curve gets to the lowest point. Although with the dose of 25 µg/kg/min Tmax begins to be a little longer than with a dose of 10 µg/kg/min, it remains shorter than at 0 µg/kg/min. We can state that the three low doses 5, 10 and 25 µg/kg/min have more effect on reducing Tmax than the larger doses.

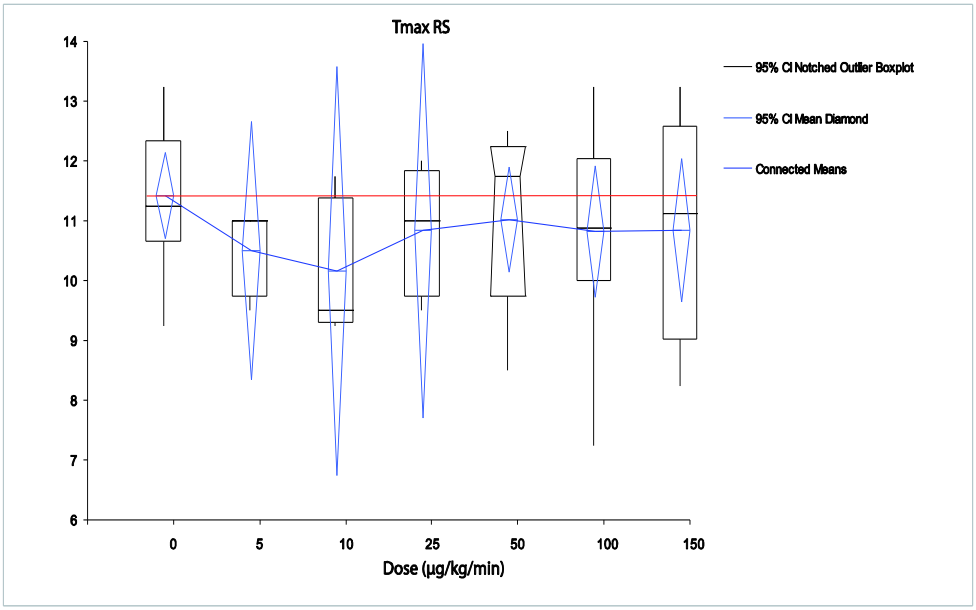

Fig.4.2.2.3 The time of maximum movement in Radial Shortening (RS) with different doses of Esmolol; the red line is the mean value of myocardial maximum movement without Esmolol.

4.2.2.4 Upslope

Fig.4.2.2.4 shows the change of upslope in radial shortening at different doses of Esmolol. With the dose of 5 and 10 µg/kg/min, the upslope is highest. From dose 25 µg/kg/min, the upslope line goes down but remains above the basic level. So the speed of contraction to maximum radial shortening is faster during Esmolol administration. Under the three higher doses of 50, 100 and 150 µg/kg/min the upslope is almost the same. The upslope of the three higher doses is smaller than that of the lower three doses.

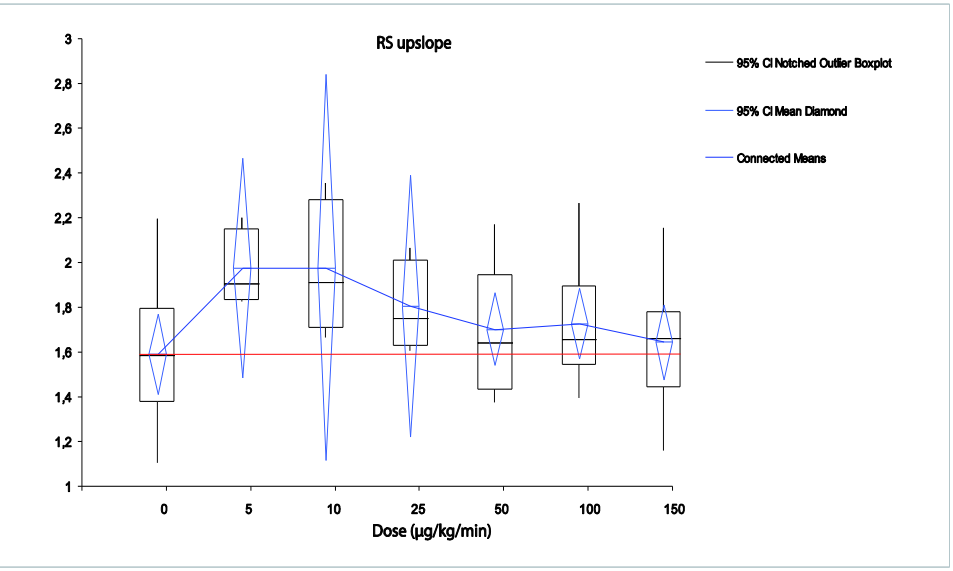

Fig.4.2.2.4 The upslope of Radial Shortening (RS) with different doses of Esmolol; the red line is the mean value of myocardial maximum movement without Esmolol.

4.2.3 Rotation

4.2.3.1 Maximum

For the rotation under different doses of Esmolol, we can also see a similar change as with circumferential and radial shortening (Fig.4.2.3.1). The rotation of the myocardium is much more evident at the doses 5 to 25 µg/kg/min. With these three doses, the maximum values are higher than with the baseline and almost keep at the same level. But the curve slips down from the dose of 50 µg/kg/min. From the dose of 50 µg/kg/min on, the medians and means of rotation drop below those of the basic dose and the three lower doses.

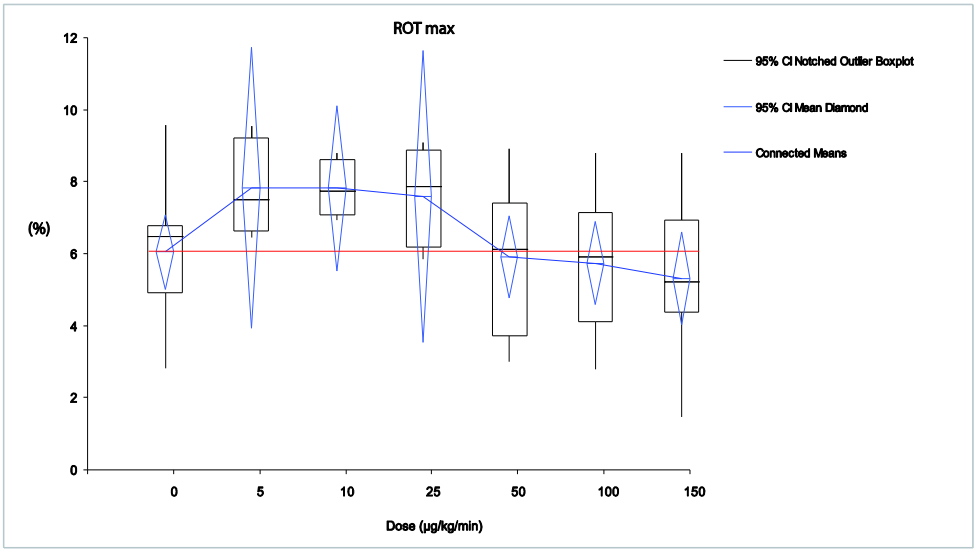

Fig.4.2.3.1 The maximum movement of myocardial in Rotation (ROT) with different doses of Esmolol; the red line is the mean value of myocardial maximum movement without Esmolol.

4.2.3.2 Area under the Curve (AUC)

The AUC of rotation of the myocardium is shown in Fig.4.2.3.2 and also coincides with the AUC of circumferential and radial shortening. The means of AUC in the doses 5, 10 and 25 µg/kg/min are visibly higher than in all other doses and so is the effect of Esmolol on the myocardium. The means of the doses 50 and 100 µg/kg/min are still higher than at 0µg/kg/min. Only the mean of the dose 150 µg/kg/min declines below baseline.

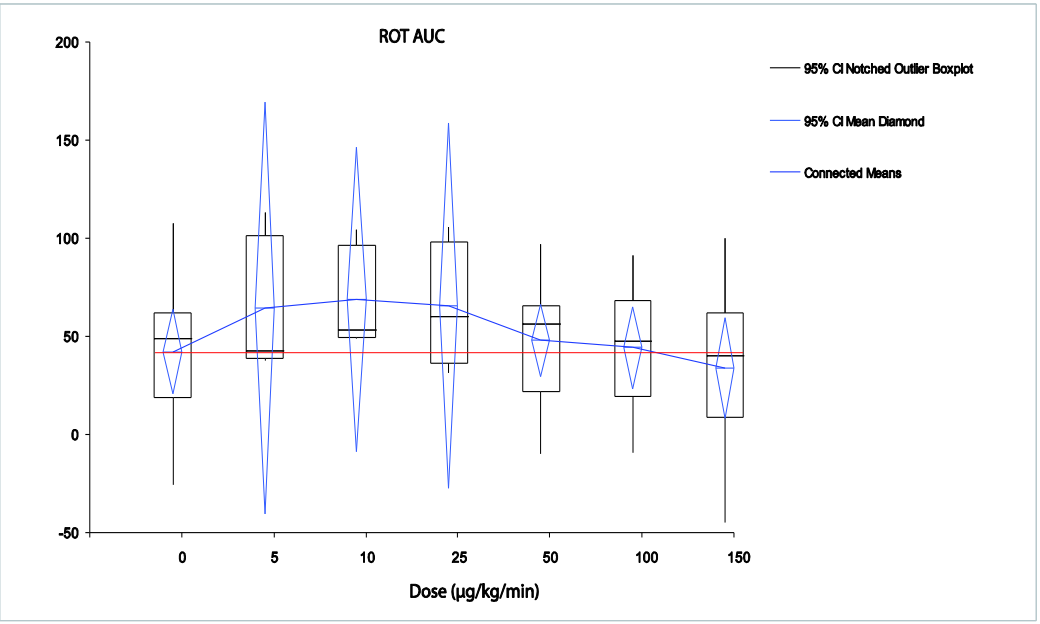

Fig.4.2.3.2 The area under the curve (AUC) in Rotation (ROT) with different doses of Esmolol; the red line is the mean value of myocardial maximum movement without Esmolol.

4.2.3.3 Time to Maximum

Fig.4.2.3.3 these results are also comparable to others' time to maximum. The time becomes shorter than at 0 µg/kg/min from 5 to 25 µg/kg/min. But from dose 50 µg/kg/min, the curve ascends and the time becomes longer than without Esmolol until 100 µg/kg/min. When dose 150 µg/kg/min was injected, the mean Tmax returns to shorter than at baseline. This is different from others' curves of time to maximum. The main part of this figure coincides with maximum and AUC of the rotation with the three doses 5, 10 and 25 µg/kg/min.

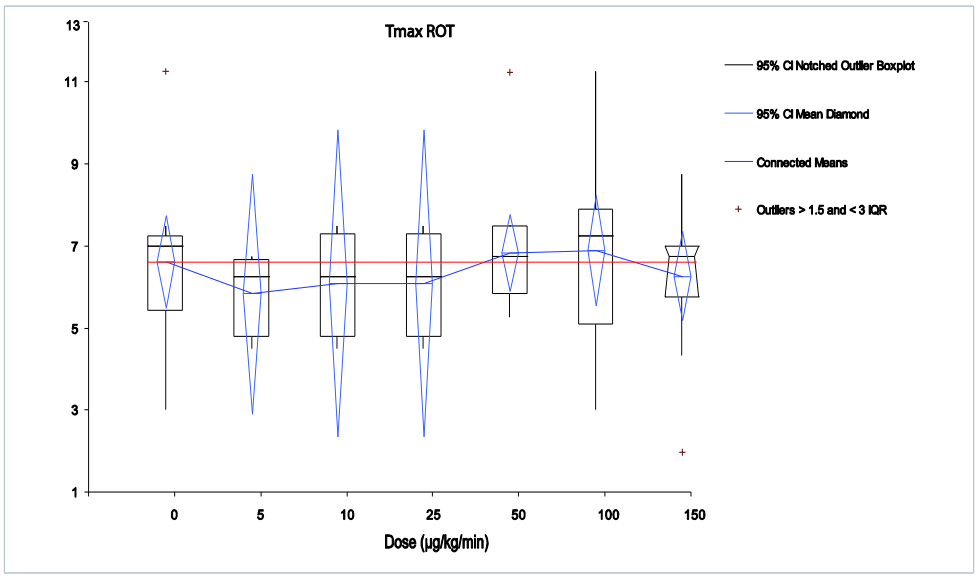

Fig.4.2.3.3 The time of maximum movement in Rotation (ROT) with different doses of Esmolol; the red line is the mean value of myocardial maximum movement without Esmolol.

4.2.3.4 Upslope

The rotation speed which is the upslope of the rotation curve was also calculated in this research project. The Fig.4.2.3.4 presents the results. The curve rises up from dose 5 to 25 µg/kg/min. The upslope of doses 5, 10 and 25 µg/kg/min are higher than the basic dose without Esmolol administration. These three doses stay at nearly the same level. From dose 50 µg/kg/min, the upslope becomes lower than the basic dose. Here a clearly biphasic mode of action of Esmolol on the myocardium with lower doses accelerating rotational speed and higher doses slowing rotation down.

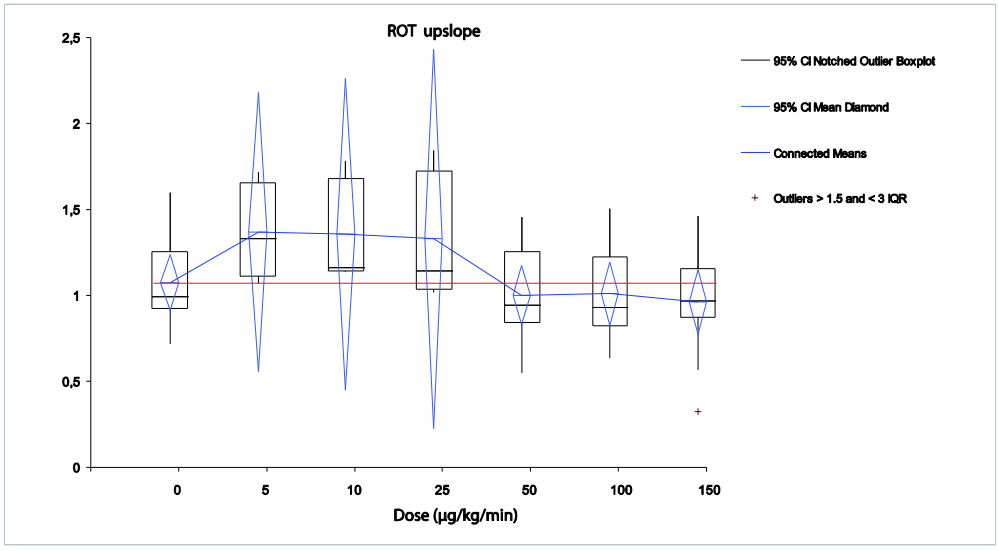

Fig.4.2.3.4 The upslope of Rotation (ROT) with different doses of Esmolol; the red line is the mean value of myocardial maximum movement without Esmolol.

4.2.4 Longitudinal Shortening

4.2.4.1 Maximum

To get the tagging data of circumferential shortening, radial shortening and rotation, we used 3D TagTrack (version 1.5.2). But Tagging on longitudinal shortening was performed by using the software 2D TagTrack (version 1.5.2). Fig.4.2.4.1 shows the analysis of myocardial maximum movement in longitudinal direction. With the dose of 5 µg/kg/min administration, the maximum of myocardial contraction drops lower than at 0 µg/kg/min. Then the curve rises with the doses 10 and 25 µg/kg/min injected over the basic dose. With Esmolol increasing to 50, 100 and 150 µg/kg/min, the myocardial maximum shortening in longitudinal direction becomes weaker than at baseline. The changes of medians with different doses Esmolol are similar to the changes of the means.

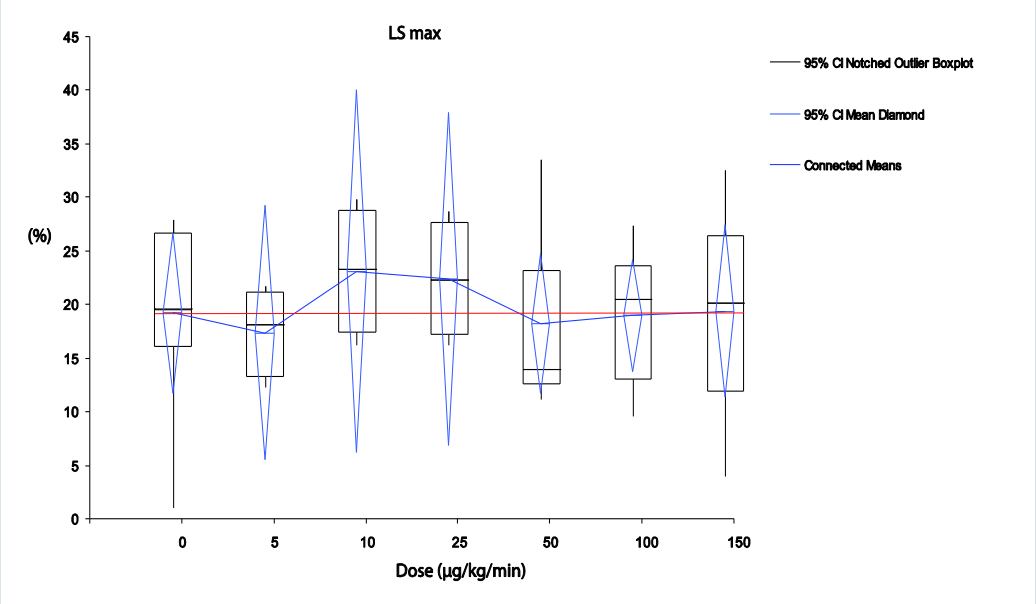

Fig.4.2.4.1 The maximum movement of myocardium in Longitudinal Shortening (LS) with different doses of Esmolol; the red line is the mean value of myocardial maximum movement without Esmolol.

4.2.4.2 Area under the Curve (AUC)

As we have mentioned before, the area under the curve reflects the work of the myocardium. From Fig.4.2.4.2, we can infer that when the lower dose of 5 µg/kg/min is given to volunteers, in average the myocardium contracts stronger. The curve of AUC in LS rises sharply and then declines constantly crossing baseline at 25 µg/kg/min. The work of the myocardial contraction becomes weaker. When the dose reaches 50 µg/kg/min and above, the means and medians lie below the baseline.

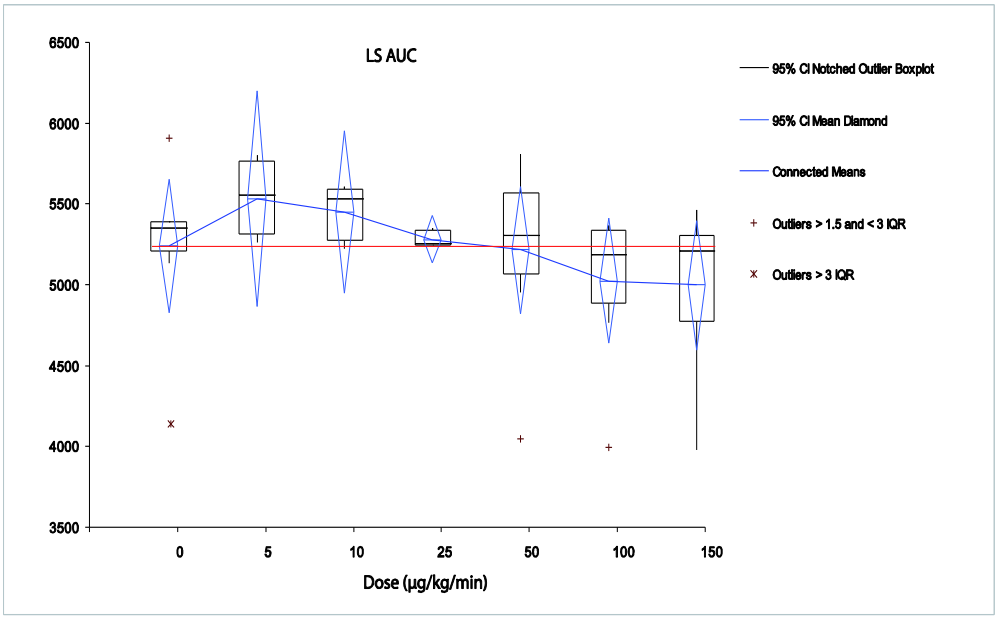

Fig.4.2.4.2 The area under the curve (AUC) in Longitudinal Shortening (LS) with different doses of Esmolol; the red line is the mean value of myocardial maximum movement without Esmolol.

4.2.4.3 Time to Maximum in LS

The curve of the time to maximum contraction in longitudinal shortening fluctuates. For all the doses of Esmolol administration, the medians and means are constantly located below those of the basic dose of 0 µg/kg/min. That reflects a shortening of systolic contraction at all given Esmolol doses.

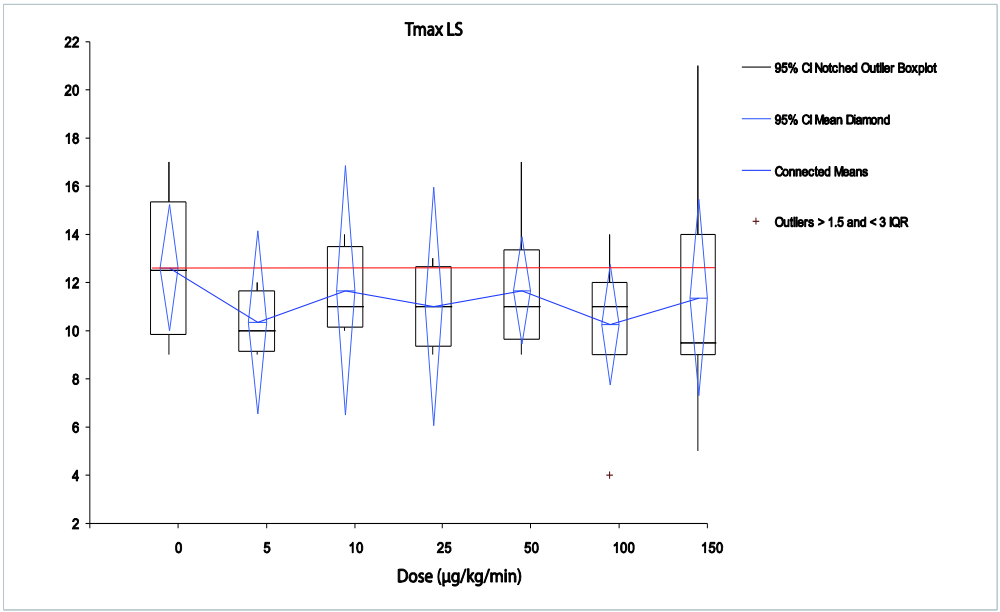

Fig.4.2.4.3 The time of maximum movement in Longitudinal Shortening (LS) with different doses of Esmolol; the red line is the mean value of myocardial maximum movement without Esmolol.

4.2.4.4 Upslope

The speed of the myocardial contraction in longitudinal shortening changes as can be seen in Fig.4.2.4.4. When Esmolol is injected at any dose, the upslope lies above base level. With doses increased to 25 µg/kg/min, the upslope reaches the vertex. From then on the means fluctuate above baseline indicating the contraction speed being a little faster than without Esmolol.

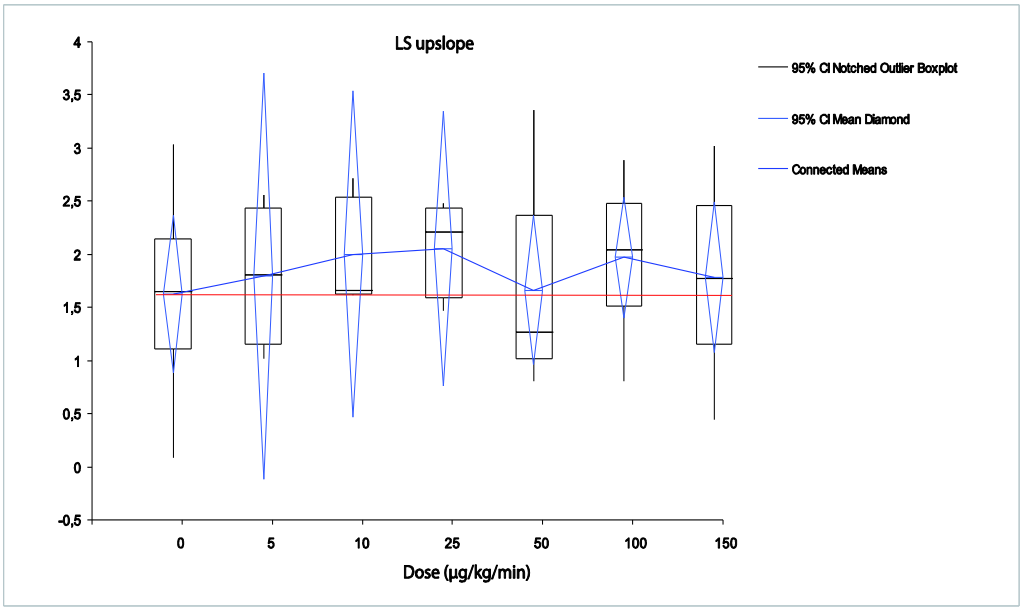

Fig.4.2.4.4 The upslope of Longitudinal Shortening (LS) with different doses of Esmolol; the red line is the mean value of myocardial maximum movement without Esmolol.

5 Discussion

5.1 Interpretation of the study results

To detect the effects of different doses of the β1-blocker Esmolol on myocardial deformation, we implemented an MRI tagging method and analysed the data of 13 healthy volunteers. In these volunteers we found differences in cardiac inotropy and lusitropy which can be divided into two fractions: Lower doses – namely 5 to 25 µg/kg/min – yielded increased circumferential and radial shortening values which we interpreted as a sign of enhanced inotropy and lusitropy. On the other hand higher doses (50 up to 150 µg/kg/min) showed unchanged or negative shortening values or respectively effects on inotropy and lusitropy when compared to the baseline values without administration of Esmolol.

In an attempt to explain these phenomenological data we applied the theory of the “inner antagonism” first introduced by P.P. Lunkenheimer (28).

Doing research in the field of hypertrophic cardiomyopathies (HCM) back in the 1960´s he remarked a decrease in septal hypertrophy in those patients treated with β-blockers but also with barbiturates. HCM patients in the operating room showed ameliorated cardiac contraction patterns during halothane narcosis. All the mentioned medications are known to exert negative inotropic effects in the normal heart. So why did they show contrary effects in HCM patients? His explanation after some years of research is based on the postulated "inner antagonism":

Nowadays it is known from studies investigating the myocardial architecture by means of Diffusion Tensor Imaging (DTI) e.g. that the orientation of myocardial cell aggregates changes during the transition from a normal to a hypertrophic heart. In the normal heart the vast majority of cells is orientated in a helical fashion spiralling around the center of the left ventricle. As the wall thickens in the hypertrophic heart an increasing number of cells are orientated in a radial fashion that means intruding from epicardial to endocardial. Furthermore the hypertrophic heart contains more collagenous tissue.

When an electrical excitation reaches the ventricular myocardium all cells start to contract. Helically arranged cell aggregates contract in longitudinal and circumferential direction. Intruding fibres contract more radially. As the myocardial mass is incompressible longitudinal and circumferential shortening leads to radial elongation and thus wall thickening. Contrarily the contraction of radially intruding cells tends to thin the ventricular wall but to lead to an elongation in longitudinal and circumferential direction. Thus intruding and helical myocyte aggregates work in a antagonistic fashion.

Negative inotropic substances like β-blockers, halothane and barbiturates seem to block the contraction of intruding myocytes more than that of helical myocytes. That is what Lunkenheimer saw back in the late 1960´s.

The mechanism that makes intruding myocytes more prone to the administration of β-blockers is still unknown and can only be speculated upon.

We think that the contraction pattern and tensile forces exerted on the cells play the key role in an explanation:

In the normal heart a vast majority of helically orientated myocytes coexists with a small minority of intruding myocytes in an interdigitated meshwork together with collagen fibres. All myocytes tend to contract in a unique pattern: after electrical excitation an isometric tension phase is followed by isotonic shortening of the contractile elements within the cell (sarcomeres) along its longitudinal axis.

Helically oriented fibres can exert this pattern easily as they are the majority. Their mainly isotonic shortening leads to an overall helical (consisting of longitudinal and circumferential) shortening of the heart which reflects systolic contraction.

Intruding myocytes tend to exert the same shortening patterns but are hindered by wall thickening which derives from helical contraction. Instead, intruding myocytes are stuck in the isometric phase throughout the complete cardiac cycle. They cannot shorten against the wall thickening forces created by contraction of the helical fibres. They are in the state of isomeric to auxotonic contraction.

This picture changes in the hypertrophic heart when the balance between helical and intruding myocyte aggregates is shifted towards the latter. The increasing number of intruding aggregates gets gradually strong enough to counteract wall thickening. Thereby intruding aggregates diminish systolic contraction of the heart and prevent unloading of the ventricle.

The hypothesis of Lunkenheimer now says that cells in the state of contraction are more prone to negative inotropic substances than relaxing or relaxed cells. As intruding cells continously are in a state of auxotonic contraction whereas helical cells can contract, unload and then relax, the intruding fibres are hypothetically more sensitive to β-blockers.

In a biochemical way this explanation makes sense: Cells that contract continously during systole (like intruding myocytes) need more calcium than cells which contract shortly in an unloading fashion. β-mimetic agents like noradrenalin augment the intracellular calcium, β-blockers prevents the intracellular calcium content from rising.

As intruding cells need more calcium β-blockers have much more impact on intruding than on helical myocytes. This effect is the more pronounced the higher the grade of hypertrophy (and by this the content of intruding myocytes). Small β-blocker doses nearly exclusively effect the intruding myocytes while with increasing β-blocker doses helical aggregates are affected as well. This is where in the presented study the initial left shift of tagging shortening curves swings back to normal and then becomes a right shift which indicates the beginning of overall negative inotropy.

To prove this hypothesis a MRI tagging study with patients of hypertrophic cardiomyopathy before and during the onset of a clinical β-blocker therapy is already initiated.

5.2 MRI tagging

5.2.1 The advantages of MRI tagging

MRI tagging is typically based upon detection of the R wave of the QRS complex. The resulting tags then follow myocardial motion during the cardiac cycle, reflecting the underlying myocardial deformation. We take MRI tagging because:

First, it can provide high spatial and temporal resolution and does not expose volunteers to potentially harmful ionizing radiation, making it ideal for serial assessments.

Second, MRI tagging can assess regional motion characteristics of the heart. Measures of regional function, such as quantification of myocardial strain and torsion, have emerged as more accurate tools for defining degrees of myocardial disease. In our study, we also need a method which can describe and quantify the myocardial movement in different directions in healthy volunteers. Because we want detect the effect on myocardium with lower doses of Esmolol. Other methods are not as accurate and prompt as we want. MRI tagging can describe the kinematics by using the terms rotation and strain tensors, the eigenvalues and eigenvectors of which allow the quantification of the maximal shortening and lengthening. Short-axis sections through the tagged volume can show the rotation and contraction; long-axis sections can display the longitudinal contraction and displacement of the myocardium. It allows accurate, unbiased determination of left ventricular anatomy and function without geometric assumptions regarding ventricular shape (29). It is a very sensitive way of the assessment of the local contraction and relaxation patterns of the myocardium in healthy and diseased states. And MRI tagging shows high precision owing to the large amount of supporting tagging data, permits us the detection of a transmural strain gradient, and is sensitive to local variations of fiber angle due to its symmetry in the circumferential-longitudinal plane (30). Originally, quantifying regional myocardial function or regional deformation required invasive surgical implantation of physical markers within the myocardium itself such as radiopaque or ultrasound makers with subsequent tracking of their motion using fluoroscopic control or echocardiography or other external imaging methods. The disadvantages of these traditional methods are invasiveness and restriction by the paucity of the physical markers. Because of their invasiveness most applications have been only used in experimental setting and were limited to animal models or patients undergoing cardiac surgery (31). Besides invasiveness, the accuracy of the implantation method is also degraded by inflammation, hemorrhage or fibrosis caused by the insertion of the foreign bodies themselves. So the original methods to quantify regional myocardial function are not suitable for our healthy volunteers.

Third, MRI is a non-invasive, normal clinical method for diagnosis and evaluation of cardiac patients. In MRI tagging non-invasive markers are created within the heart tissue by locally induced perturbations of the magnetization with selective radiofrequency saturation of multiple,

thin tagging planes in a plane perpendicular to the imaging plane prior to image acquisition. These perturbations then produce regions of reduced signal intensity that appear as dark lines superimposed on myocardial tissue in the depicted images. From our study, we can introduce MRI tagging into clinic for myocardial regional deformation to detect underlying regional dysfunction even ejection fraction is normal.

5.2.2 Comparison with other clinical imaging modalities to display myocardial motion

Various imaging techniques such as magnetic resonance imaging, echocardiography, computed tomography (CT) and angiography can detect alterations in the deformation of the myocardium. Among these methods used to assess the myocardial motion or myocardial function, two dimensional speckle tracking echocardiography (2D-STE) was introduced as a used non-invasive approach to measure left ventricular deformation mechanics and is nowadays wildly used in clinic.

This method not only allows to measure longitudinal deformation and strain, but also to assess myocardial rotational and torsional mechanics as the MRI tagging method does. In contrast to 2D-STE, MRI tagging is limited by inherent low frame rate acquisition, high cost, complex data analysis and limited availability (32). Time for patient setup (placement, ECG tracing, coil connection) is also minimally longer than for 2D-STE. Patients with claustrophobia or metallic implants (pacemakers, cardioverter-defibrillators) must not be examined by MRI. Compared to echocardiography, another potential limitation of MRI tagging is low specificity in the subendocardium (33). We can also take 2D-STE in our study. But we still choose MRI tagging to detect because of the inherent advantages of MRI tagging shall not be ignored.

For example, images of MRI tagging can be acquired with good and reproducible image quality independent of the examiner and the patient's condition (e.g., emphysema, adipositas), because no imaging window is needed (34). This has to be interpolated from serial examination under differing conditions, as in our study, inter- and intra-observers variability are lower in MRI tagging than in 2D-STE.

Another advantage of MRI tagging compared with the older techniques is that it allows a higher density of markers and full functional imaging of intramural myocardium. MRI tagging has a transmural resolution which allows to differentiate subendocardium, midwall and subepicaridum. Using MRI tagging, the endocardial border can easily be detected and separated from intracavitary blood because a high natural contrast between blood in motion and the myocardium exists. Good spatial resolution, high signal-to-noise ratio, and sharp contour delineation in MRI images meet the requirements for our accurate quantitative analysis. Tethering effects from

akinetic nonviable segments on viable but dysfunctional segments may explain lower accuracy of echocardiography in akinetic segments. In contract segments of severe hypokinesis that improved by >5% can be detected by MRI tagging (33). To estimate apical rotation, the 2D-STE ability is significantly lower than that of MRI tagging because of the inability of 2D-STE to visualize the true left ventricular apex in a significant number of normal and diseased subjects. Comparing end-diastolic internal dimensions among the available 2D-STE apical cross-sections with serial consecutive 10 mm MRI tagging left ventricular cross-sections, Goffinet (32) found that 2D-STE images were acquired at the real left ventricular apex in only 10% of the subjects.
Comparing to MRI tagging, echo technique, using ultrasonic crystals and ultrasound imaging, had the disadvantages of a lack of physical markers. Additionally ultrasound images had a relatively low signal-to-noise ratio (35). Even when these imaging methods work well for determining the position and movement of the endocardial and epicardial contours, they do not allow direct assessment of the intrinsic contractility of the myocardium. Thus, compared with older 4-level echocardiography scoring systems, more segments with functional changes would likely be detected by MRI tagging which we choose for our study.

5.2.3 Technical considerations to improve MRI tagging

Although there are many advantages of MRI tagging, we can not ignore that fading of the tag lines close to end-diastole, as a result of T1 tissue relaxation and the imaging radiofrequency, has limited its application to the systolic part of the cardiac cycle. The contrast between the tissue and the tagging lines decreases considerably during the later phases of the cardiac cycle. We used high field strength magnets (3T) for tagging acquisition to reduce the tag fading problem. Achieving myocardium tagging at higher field strength appears to provide a better contrast to noise ratio (CNR) and improve tagging persistence. This is because of a higher baseline signal to noise ratio (SNR) provided by 3T systems and prolongation of myocardial T1. Both of them improve the contrast between the tissue and the tagging lines at end-diastole during the process in our study (36).

In fact, in order to reduce tag fading due to T1-relaxation, another improvement CSPAMM using segmented k-space was also implicated and used in our study (37). This helped to improve the tagging contrast, especially in the later phases of the cardiac cycle. The tagging grid became the predominant signal, with hardly any contribution from the anatomic background which can suppress the deformation of the tag lines due to T1 relaxation and also the displacement due to fat. Even though there was a marked improvement in tag contrast, the contours of the tag lines are comparable to those of normal SPAMM tagging. Another advantage of CSPAMM is that it

can be easily extended to all three dimensions by tagging planes in three orthogonal directions. This characteristic satisfies our requirement of acquiring 3 dimensional data. All the improvement in contrast of CSPAMM greatly enhances the possibility of using automatic tracking techniques. The primary drawback of the CSPAMM technique in our study is that it doubles the acquisition time and thus the breath-holding time, which may result in the mis-registration of the images to be subtracted.

However, our overall reduction of imaging time with CSPAMM is possible. We applied a segmented echo-planar imaging sequence that allows the acquisition of systolic and diastolic grid-tags within a single breath-hold (38). So the total acquisition time could substantially be reduced since significantly fewer breath-hold measurements (one for each slice under examination) had to be performed to obtain data covering the whole left ventricle. However the presented technique also exhibits limitations when assessing motion of very thin structures such as the right ventricle or remodeled post-infarct scar tissue. This is related to the limited spatial resolution leading to partial volume effects and differences in EPI-related image distortions between the three line tag encoded datasets. But by supplying a higher spatial resolution and a shorter EPI echo train one could solve this problem at the cost of a longer scan time resulting in more breath holds.

MRI imaging is further influenced by the distance of the object from the receiver coil and another possible source of error in MRI imaging is the presence of blood and myocardium in the same voxel (34). In order to improve the suboptimal temporal resolution within the ECG cycle, the traditional way of decreasing scan time by utilizing stronger and faster gradients is limited because of scanner noise and, more importantly, peripheral nerve stimulation. Even with the current hardware we do not use the full performance of the gradients, in order to create measurement tolerable for patients. Our possible solution to this problem is the application of faster pulse sequences (e.g., segmented Echo Planar Imaging (EPI) based approaches as executed in this study) and/or more sophisticated view-sharing techniques, which can be used to improved temporal resolution within the ECG cycle (39).

5.2.4 HARP

During post processing, we exerted the harmonic phase (HARP) method to analyze the MRI tagging data. HARP analysis is faster regarding processing time than previous techniques. The reason we used HARP is that it can so supply automated analysis of motion tracking on myocardium through all acquired time frames with minimal user interaction. Its potential in clinical cardiology depends on the demonstration of its sensitivity to small changes in

myocardial strain during pharmacological stress testing, e.g., and on its ability to accurately index regional wall motion abnormalities (40). So we used HARP in a setting deviated from strings testing in an opposite way one could call ‘rest testing’ by administering β-blocker.

The HARP method calculates the spatial phase for each pixel in the periodic tagging pattern. This HARP imaging approach allows fast visualization and to calculate the deformation directly by calculating the regional spatial frequency of the tagging pattern and comparing it with the undeformed frequency. HARP is based on the fact that the inverse Fourier transform action creates a spectral peak in the Fourier domain. This produces a complex image with phase linearly related to a directional component of tissue displacement. That permits the isolation of tag motion components giving the possibility to make the analysis of regional function completely automatic. The phase change is related to the in-plane motion of the myocardial tags. If there is no motion, the phase of the sinusoidal tag pattern remains linear. If there is motion, the sinusoidal tag pattern deviates from linearity in its phase (38).

During post processing of our study tagging data while tracking the myocardial motion with HARP method, some incorrectly tracked points appeared in the images. Unfortunately this problem could not be solved by refinement. But it could be avoided by choosing points which are not too close to the myocardial boundaries (41).

With the MRI tagging method, a large variety of parameters describing cardiac deformations can be extracted from the acquired data. Maximum and time course of shortening pattern were examined in this initial study. Examples of other parameters such as rotation and left ventricular torsion, as well as their derivatives describing velocities can also be detected. Additionally MRI tagging offers the capability of combining functional and anatomic measures to obtain a more comprehensive assessment of cardiac function. In clinic, MRI tagging can be of great value for the detection of myocardial ischemia during stress testing. Similarly, it might provide fast and accurate quantification of functional recovery in stunned or hibernating but viable myocardium. It might also be useful for studying dynamic changes in regional LV function after acute infarction by allowing serial quantitative examinations over time. Alterations in left ventricular torsional deformation may be important in several pathological states. Because HARP has the potential for other applications in any tracking motion technique, it allows for rapid non-invasive assessment of twist mechanics in the human heart, in different myocardial segments.

5.3 β-blockers

During last three decades, the position of β-blockers has evolved from contraindication to established treatment and has changed the management of heart failure dramatically. Heart

failure patients seen in clinical practice who are prescribed β-blockers have better outcomes than those who are not provided this therapy, even after adjusting for age, sex, ejection fraction, cause of heart failure, type of dysfunction, year of prescription, and concomitant use of other medications shown to influence prognosis (such as ACE inhibitors) (22). In clinical trials β-blockers have been shown to lead to long term improvement in patients with heart failure, in terms of reduced hospitalisation, improved left ventricular function, slowing of heart failure progression, and increased life expectancy. Although initially there can be some clinical deterioration, even these patients can gain long term benefit.

5.3.1 Mechanisms of β-blocker action

β-blockers differ with regard to their pharmacologic properties, including β_1 and β_2-adrenergic receptor selectivity, intrinsic sympathomimetic activity (ISA) and vasodilatory properties. Commonly β-blockers are divided into three generations of agents. First-generation β-blockers, such as propranolol, exert equal blockade of β_1 and β_2-adrenergic receptors, and are therefore described as non-selective β-blockers. The second generation exhibits higher affinity binding to β_1-receptors than to β_2-receptors, and are termed selective β-blockers. The extent of selectivity of these agents (e.g., metoprolol, atenolol, bisoprolol, esmolol) is not absolute and ranges widely among the agents. β_1-selectivity implies greater safety in treatment of patients with obstructive pulmonary disease, diabetes mellitus or peripheral vascular disease because β_2-agonist effects (bronchodilation, vasodilation) are presumably maintained. The third-generation β-blockers (e.g., carvedilol) are distinguished from the earlier classes of β-blockers by their ancillary vasodilating activity. These agents appear to provide vasodilation primarily through their blockade of the α_1-receptor, which contributes to regulation of endothelial function and vasoconstriction in peripheral blood vessels.

The rationale for the use of β-blockers in heart failure patients is based on observations that sympathetic efferent neuronal activity is increased in heart failure and that this sympatho excitation has an independent prognostic value. β-blockers inhibit sympathetic outflow centrally, slow heart rate and reduce the renin-angiotensin-aldosterone system activity by inhibiting renin release. These drugs may provide cardiac protection in heart failure via blockade of post-junctional β-adrenergic receptors on cardiac myocytes. In addition, the improvements by β-blocker include reduction in oxygen consumption and metabolic demand, reversal of β-receptor down-regulation observed in the failing heart, anti-ischemic and anti-arrhythmic effects, anti-hypertensive and correction of abnormal intracellular calcium handling. A further rationale for anti-adrenergic treatment is inhibition of direct cardiotoxic effect of noradrenaline. β-blockers

may also improve diastolic filling, thereby enhancing perfusion and metabolism. The increased nitric oxide release induced by β-blockers may cause an additional improvement of early relaxation (42). β-blockers can lower the risk of worsening heart failure significantly. This effect is caused by the β_1-receptor blockade, and involved mechanisms may be related to autonomic activity, receptor kinetics, myocardial energy balance, electrophysiology, neuroendocrine deactivation and ventricular remodelling. Another mechanism by which β-blockers may be beneficial is through the antagonism of pre-junctional β_2-adrenergic receptors, which protect the heart from the surges in sympathetic nervous activity that facilitate neural norepinephrine release and from vagal withdrawal that may trigger ventricular fibrillation and sudden death (43).

5.3.2 The characters of the β-blocker Esmolol

For our research, we choose the second generation β-blocker Esmolol although many kinds of β-blockers are used in clinic. Because Esmolol is a cardio-selective β_1 adrenergic receptor blocking agent without significant intrinsic sympathomimetic activity, vasodilatory capabilities, significant membrane stabilizing activity and β_2-agonistic effects. And most importance is that it has a rapid distribution half-life of 2 min and short duration of action with an elimination half-life about 9 min (44). Steady-state blood levels are maintained during infusion, but decrease rapidly after termination of the infusion. After termination of infusion, substantial recovery from Esmolol is observed in 10-20 min. At 30 min after the discontinuation of Esmolol infusion, all of the hemodynamic parameters will return to pre-treatment levels (45). Because the half-life of Esmolol is short, it is easy to control and much safer for our research. Under the dose of 300 μg/kg/min of Esmolol, infusions may be continued for as long as 24h (45). So it is better and safer for us to detect different effects on myocardium function using different doses of Esmolol. Because of the characteristic of Esmolol, it can also reduce the detection time for every volunteer at different doses.

Esmolol is a phenoxypropanolamine that is metabolized rapidly by esterases in the cytosol of red blood cells. Metabolism of Esmolol results in the formation of the corresponding free acid and methanol. Its acid metabolite has only 1/1000 β adrenergic-receptor blocking activity of Esmolol (46). The acid metabolite has an elimination half-life of 3.7 h and is excreted in the urine with a clearance that is approximately equivalent to the glomerular filtration rate. Excretion of the acid metabolite is significantly decreased in patients with renal disease, with the elimination half-life increased to 10-fold that of normal subjects, and plasma levels considerably elevated. Esmolol has been shown to be 55% bound to human plasma protein, whereas the acid metabolite is only 10% bound (45). Metabolism of Esmolol is not limited by the rate of blood flow to metabolizing

tissues, such as the liver. Total body clearance in man was found to be 20 l/kg/h, which is greater than cardiac output. If intolerance to β-blocker develops, termination of the Esmolol infusion should result in rapid reversal of the pharmacologic effects. The rapid reversal of hemodynamic effects closely paralleled the rapid decline of Esmolol blood concentrations. So among patients who may benefit from β-blockers, but also are at risk for adverse effects, Esmolol has the advantages of rapid adjustment of hemodynamic effect as well as a short duration of effect following discontinuation.

Esmolol produces clinically useful decreases in blood pressure and left ventricular contractility similar to other β-blockers. Because these effects typically result in reduced myocardial oxygen consumption, Esmolol can produce beneficial effects in patients with ischemic heart disease and improve cardiac index, ejection fraction of the patients. In human electrophysiology studies, Esmolol produced effects typical of a β-blocker: a decrease in the heart rate, prolongation of the sinus node recovery time during normal sinus rhythm and during atrial pacing, and an increase in antegrade Wenckebach cycle length.

5.3.3 Detection of benefit of low doses of β-blocker Esmolol from our study

Based on our results, we can conclude that in the modern insights, the lower doses of β-blockers may be much more effective than the higher doses, especially in clinic when the patients are frailer, elderly and can not tolerate the higher doses.

But why do low doses of Esmolol or other β-blockers have much more positive effect on the myocardium? Our group inclines to one opinion that different myocytes which are aggressive in different geometrical alignment within the ventricular myocardial mesh have differing sensitivity to Esmolol. In the former chapter, we discussed that the ventricular mass is organized in the form of meshwork, with populations of myocytes aggregated in a supporting matrix of fibrous tissue, with some myocytes aligned obliquely across the wall so as to work in an antagonistic fashion compared to the majority of myocytes, which are aggregated together in tangential alignment (11-13). The disparate working conditions for the tangential and oblique transmural components of the myocardium would generate two types of force signal. The tangential myocytes are relative to the thickness of the ventricular walls and responsible for overall constriction of the ventricular cavity. While the myocytes orientated with their long axes running obliquely from the epicardium to the endocardium partially counteract to the mural thickening (13). With respect to global ventricular function, this oblique arrangement produces an antagonistic mechanism, which serves to stabilize ventricular shape and to terminate systolic mural thickening. The presence of the greater amount of myocytes being aggregated tangentially, while

a smaller, yet significant, number of myocytes aligned with oblique orientation, all of them acting synchronously, serves to put the wall itself under stress from all directions, thus providing different movements of myocardium and presenting different myocardial function. The thicker the wall becomes at end-systole, the more the myocytes are inclined relative to the short axis. Hence, the greater is the increment of the auxotonic forces as the myocytes are deviated in an oblique direction from the epicardium to the endocardium (4), and the more they counteract to the systolic mural thickening. We speculate that Esmolol at low doses exerts an instantaneous selective action, which constrains the forces engendered by those myocytes which are aggregated with their long axis oblique relative to the short axis of the ventricular wall. These aggregated myocytes are more sensitive to the action of β-blocker than the prevailing tangentially aggregated myocytes engendering the constrictive activity. According to this hypothesis, with low doses of Esmolol, the oblique aggregated myocytes are restrained. And auxotonic forces produced by oblique myocytes are weaker than the contract forces from tangential myocytes which are still active at low doses of Esmolol, so that result to the stronger contraction of the myocardium. Lunkenheimer's research (47) has also confirmed this point that the obliquely orientated myocytes, which contract auxotonically, are the primary target of Esmolol when this drug is given in low doses using implanting needle probes during heart surgery. As former literature reported, in clinic there is also a trend to use low doses of β-blockers to attenuate β-blockers' negative effect such as a drop in systemic systolic pressure, low heart rate resulted of high doses which attenuate those prevailing tangential aggregates of myocytes that sustain ventricular ejection.

But why are the oblique myocytes more sensitive to β-blockers than the tangential myocytes? We have another hypothesis relative to the different distribution of β receptors. In heart failure patients, there is a selective down-regulation of β_1 receptors while myocardial β_2-receptors are not changed (48). Down-regulation is thought to be a secondary phenomenon to overstimulation of the β_1-adrenergic receptor. So we can imagine that there is a possibility that the distribution of β_1 and β_2 receptors on myocytes which are aggregated obliquely is different from tangential myocytes. Esmolol is a kind of short active β_1-blocker. If β_1-receptors stay much more on oblique myocytes than on tangential myocytes, the myocytes which are aggregated in oblique should be more sensitive to lower doses of Esmolol. So with lower doses of Esmolol blocking the oblique myocytes, the tangential myocytes will make more work. If this assumption is right, it can also explain our research results. But unfortunately we didn't search any literature to support our viewpoint. So in the future, we can design an experiment to detect whether this assumption that different distribution of β-adrenergic receptor is right or not.

In conclusion, our present investigation provides further insights into the effects of initiation of β-blocker therapy in heart failure. We have shown that Esmolol at low intravenous doses increases myocardial function without relevant negative inotropic effects. Low intravenous doses of a β-blocker may accordingly represent a beneficial therapeutic principle in addition to conventional therapy for patients with heart failure who are frail and can't tolerate the high doses of β-blocker.

5.3.4 Support from clinical reports

Last century, many people thought higher dose of β-blocker produced a more beneficial effect than lower dose. But sometimes the effectiveness of β-blockers in real-world practice is uncertain. Viskin et al (49) found that 89% of patients who were discharged from the hospital and prescribed a β-blocker regimen received doses 50% or less of the doses shown to be effective in randomized clinical trials. Other research (50) findings also suggest that dispensing of high-dose rather than low-dose β-blocker therapy was associated with more than a 50% greater risk of admission for heart failure in this cohort. It is uncertain whether the patients who are elder, frailer and with conditions (such as chronic obstructive pulmonary disease) can tolerate the higher doses of β-blockers. In addition, treatment with β-blockers is frequently prescribed at lower doses than those investigated in clinical trials, probably attributable to concern about its tolerability (51). Tandon's (22) data suggest that even low dose β-blockers are associated with improved survival in nontrial heart failure patients.

Current European guidelines on heart failure treatment recommend initiation of β-blocker therapy with a small dose, and a gradual increase in dosage until target tolerated dose used in large clinical trials is achieved.

Compared to the randomized trial setting, which use careful up-titration schedules to reach target doses, in clinical practice, a lower percentage of patients may actually receive target doses, and many patients only receive medium or low doses. In Puneeta's research (22), only 18% of patients prescribed β-blockers achieved the target doses in the β-blocker trials. Daniela's study (52) provided more information on the benefit of low dose β-blocker therapy. Patients who received lower dose β-blocker therapy (<50% of trial dose which he defined) had a similar survival to those receiving higher doses. This may encourage clinicians to prescribe low doses of β-blockers when high doses can't be achieved.

Bristow's (53) paper referred that low- to moderate-dose β-blocker with metoprolol can restore downregulated β1-adrenergic receptors in failing myocardium as a result of idiopathic dilated cardiomyopathy (IDC) and might be preferable for restoring exercise responses. This is because

low-level competitive β-blocker may be overcome during exercise by evoked norepinephrine release, allowing for full chronotropic and inotropic stimulation of the reconstituted β-receptor pathway.

Rochon's finding (50) suggest that use of a low dose β-blocker may further lower the risk of admission for heart failure among survivors of myocardial infarction. Higher doses are associated with a greater risk of admission for heart failure. His results provide some assurance in clinic that patients receiving low doses of β-blocker (who are probably unable to tolerate higher doses) should continue their therapy. Furthermore, the potential survival benefit associated with the use of low dose β-blocker therapy may encourage physicians to use these drugs in frail older people who might not be prescribed them otherwise. Although his results do not provide definitive evidence on the best dose, they support a low dose at first and gradual increases as tolerated.

In Felix's paper (54), his group disclosed that for patients with severe decompensated heart failure intravenous application of low doses of celiprolol was associated with no detrimental hemodynamic effects, and that this treatment evidently ameliorates myocardial energy demand without relevant negative inotropic effects. His investigation provides further insights into the effects of initiation of β-blocker therapy in severe heart failure. Celiprolol at low intravenous doses induces a decrease in heart rate without relevant negative inotropic effects. Low intravenous doses of a β-blocker with vasodilating properties may accordingly represent a beneficial therapeutic principle in addition to conventional therapy for patients with severe heart failure in which reduction of heart rate is regarded necessary for hemodynamic stabilization and reduction of myocardial energy demand.

Wikstrand and his group (55) implemented a study to detect the difference between high and low doses of one kind of β-blockers. He found that during 3 months of therapy with β-blocker, the heart rate was reduced to a similar degree at both high and low doses. During the titration phase, plasma concentration of β-blocker at the three-month visit suggested that the patients in the low dose group were more sensitive to β-blocker than the patients in the high dose group.

Barron (56) compared the data of clinical patients and observed that the actual dose of β-blockers prescribed at the time of discharge from the hospital was much lower than the doses used in randomized controlled trials, confirming the observations made by Viskin. The most important observation of this study was, however, that treatment with lower doses of β-blockers was associated with a significantly greater reduction in cardiovascular mortality than treatment with higher doses.

So from our results and former clinical reports, we can conclude that low doses of β-blockers may supply much more benefit to cardiac patients than higher doses.

5.4 Age

Our study included 13 healthy volunteers with a median age of 36 years (age range from 29 to 41 years). Actually they belong to young group. So we did not detect the different effect of β-blocker Esmolol on different ages.

But in the early days, advancing age was a predictor of shortened survival in individuals with heart failure (HF), with a 27% increase in mortality per decade of advancing age in men and a 61% increase per decade in women (57). Because of an increased rate of complications and worse basic health situation of the elderly patients, there sometimes is higher mortality and an unideal medical effect that can be seen in older patients compared to the younger ones. Some researches show that the mortality risk reduction decreases with age from 71% in younger patients to $\leq 21\%$ in the older ones (52).

Most of the elderly patients with heart failure also have additional complications and a reduced basic health situation. So the advanced age is both a univariate and multivariate predictor of poor tolerability of β-blockers as diastolic hypotension, bradycardia, presence of obstructive airways disease, low ejection fraction or worsening failure symptomatology might occur (22, 58). There are strong trends towards use of higher doses of β-blockers in those patients who are younger, have less severe symptoms (NYHA classes I and II), have higher ejection fractions, have higher systolic blood pressure and are also prescribed ACE inhibitors or dihydropyridine calcium channel blockers (22). Furthermore, doses in clinical trials, where patients are younger and are force-titrated to target dose, are higher (58). Tabassome's research (59) finds that patients tolerating only low doses were significantly older patients with more severe NYHA functional class and higher frequency of co-morbidities. Nevertheless, the dose achieved in everyday clinical practice demonstrates that therapeutic doses of β-blocker therapy can be achieved even in an elderly heart failure patient cohort. A previous meta-analysis in patients with systolic HF has shown that older patients (>60–70 y) derive as much benefit from β-blockers as younger patients (60). The SENIORS study (8) has recently reported on the efficiency of β-blocker therapy with the β_1-selective vasodilator Nebivolol in a systolic and diastolic HF population older than 70 years of age. The primary end-point of death and cardiovascular hospitalisation was reduced by Nebivolol compared to placebo. This agent appeared to be generally well tolerated in the elderly patients. Moreover, elderly patients with co-morbid conditions in which β-blockers may be considered relatively contraindicated also appeared to tolerate β-blocker well.

Therefore, based on the above observations, elderly HF patients should not be denied β-blocker therapy because of concerns regarding tolerability.

In addition, treatment with β-blockers is frequently prescribed at doses lower than those investigated in clinical trials, probably attributable to concerns about tolerability in the elderly. Some researches (61) report that there may be a decreased response to β-blocker therapy in the elderly patients. Altered drug actions in older people are mainly attributed to age-related pharmacodynamic and pharmacokinetic changes, such as alterations in receptor density and sensitivity, endocrine activation and changes in the balance of the autonomic nervous system. Such changes appear in particular after the age of 70 years.

But from a lot of research results, we can state that β-blockers are of benefit to younger patients as well as elderly patients. Overall good tolerability in patients should be thought to be appropriate by their treating clinician for β-blockers despite advanced age. Even in the extremely elderly (>80 y), there is little diminution in tolerability (58). Although elderly patients are at higher risk of hypotension, bradycardia and other side-effects of β-blockers compared with younger patients. In clinical trials, β-blockers have been shown to lead to long term improvement in both younger and elderly patients, in terms of reduced hospitalisation, improved left ventricular function, slowing of heart failure progression and increased life expectancy (19). Both younger and elderly HF patients should receive β-blocker therapy.

SENIORS (8) shows both a significant overall treatment effect and a virtually identical point estimate of risk reduction for younger or older patients with low and preserved ejection fraction. This is the best evidence to date of a treatment likely to be effective in a substantial proportion of the elderly population with heart failure who have a broad range of ventricular dysfunction.

5.5 Gender

We have 13 healthy volunteers involving in our study including 6 male 7 female. From our study we did not find the obvious difference effect of β-blocker Esmolol on different genders. Neither there was difference on MRI tagging between male and female volunteers. Epidemiological studies have suggested sex-related differences in the incidence and the prognosis of heart failure (57). Regardless of all of the baseline clinical differences, women are at lower risk for all cause mortality, cardiovascular death, non-cardiovascular death, and death from heart failure.

The underlying mechanisms of gender difference and hormonal effects on cardiac remodelling remain poorly investigated, but could be related to differential constitutive nitric oxide synthase regulation and its effects on the myocardium and coronary vasculature (62). This could manifest

at early stages of response to load or injury as differential behaviour of myocardium actions between men and women.

Apart of the prevalence of heart failure and different cardiac hypertrophy and dysfunction, some studies have suggested possible sex-related differences in adrenergic receptor sensitivity or post-receptor effector activity. Mills (63) found that women showed greater post-receptor adenylate cycle activity independent of the β-receptor. When these differences were investigated, the gender-related differences in β_2-receptor sensitivity were no longer evident. Also his research reported that black women had reduced β_2-receptor sensitivity in the luteal phase compared to the follicular phase, whereas white women showed no significant change. Black women had lower β_2-receptor density values than white.

There are also data that suggest sex-related differences existing in the pharmacokinetics and pharmacodynamics of β-blockers, resulting in greater drug exposure, greater reduction in exercise heart rate and systolic blood pressure in women (64). Simon et al. (65) implemented a research project on different sex (515 female and 2132 men) in the Cardiac Insufficiency Bisoprolol study. The results show that women who were treated with Bisoprolol had a higher unadjusted protective effect than did men for all-cause mortality. Kaplan-Meier analysis revealed a lower percentage of death among women treated with Bisoprolol compared with men (6% versus 12% at mean follow-up, respectively, P=0.01), whereas in the placebo group, the reduced rate of mortality in women was not significant (13% versus 18%, respectively, P=0.10).

So Simon states that female sex was a significant factor of survival regardless of baseline clinical profile and treatment. Although he confirmed better survival for women compared to men, this difference was predominantly noted in the undefined etiology, and no difference in survival was seen between women and men in the nonischemic (66).

Some other researchers' analysis presents other findings. Packer and colleagues found that the reduction in mortality rates of heart failure was not sex related with Carvedilol (67) even in the nonischemic cardiac disease. While in the CIBIS II study, which was a double-blind trial that randomized 2647 patients with symptomatic NYHA class III or IV HF and LVEF<35% to Bisoprolol or placebo, as well as in COPERNICUS, a double-blind trial that randomized 2289 patients with severe HF and LVEF<25% to Carvedilol or placebo, the analysis results (68) showed that a very similar survival benefit was noted in women and men. Here a difference between women and men was not evident.

But the interaction between sex and Metoprolol therapy analyzed in the MERIT study gave an opposite standpoint. Subgroup analysis showed a significant reduction in mortality rates for men treated with Metoprolol but not for women (69).

There is not only difference on epidemiological and medication between male and female, but also different gender has an influence in magnetic resonance values of the myocardium. When the researchers investigated the values in MRI, they found greater left ventricle volume and mass in men, before and after adjustment for height and body surface area (BSA), excluding symptomatic cardiovascular disease and hypertension (29). End-diastolic volume (EDV) and end-systolic volume (ESV) were also significantly greater in men than in women. Gender difference impacts the results of different methods of physical examination. Gender specific values for normal cardiovascular MRI left ventricle mass are lower than reported about M-mode-derived values obtained from 864 healthy adults drawn from the same Framingham Heart Study (FHS) Offspring cohort (70).

In conclusion there are various opinions on the different prevalence, myocardial change, medical effect and medical detection in myocardial disease between women and men.

6 Summary

Background: The heart as one of the most important organs in the human body has its specific anatomy characters. The ventricular mass is organized in the form of meshwork, with populations of myocytes aggregated in a supporting matrix of fibrous tissue. The major myocytes are aggregated together in tangential alignment compared to the antagonistic myocytes which are aligned obliquely across the wall from the epicardium to the endocardium. The disparate working conditions for the tangential and oblique transmural components of the myocardium generate two types of force. The oblique myocytes can engender the auxotonic forces which is opposite to the forces produced by the tangentially aggregated myocytes and counteracts to the thickening of the ventricular. On the basic thesis that the two groups of aggregated myocytes produce two opposed forces: one contracting the myocardium the other counteracting in the thickening ventricular, we designed the research on different doses of short action β-blocker Esmolol with varying effect on myocytes and myocardial function.

MRI-tagging is typical a magnetic resonance technology to detect regional cardiac function such as quantification of myocardial disease. Complementary spatial modulation of magnetization (CSPAMM) is one of the MRI tagging technologies which can minimize the tag fading due to T1 relaxation and is able to tag and assess the whole heart. It is a very sensitive way for the assessment of the local contraction and relaxation pattern of the myocardium in healthy and diseased states.

Method: The whole process of our research study includes 13 volunteers (6 male, 7 female) in Berlin with a median age of 36 years (age range from 29 to 41 years). During the entire process, all the volunteers were monitored by ECG, BP, SpO_2 every 3 min. The whole doses (0, 5, 10, 25, 50, 100, 150 µg/kg/min) of Esmolol were successively injected during a period of approximately 12-13 min. After every injected dose injected we waited for about 4 min for the effect of Esmolol. Then the MRI scan began. After acquiring the MRI-tagging data, we applied a method called harmonic phase (HARP) with the softwares of 3D or 2D TagTrack to analyze the data. HARP analysis is currently the most widely used method for strain quantification since it is highly automated and limits both analysis time and subjective interference. For statistics we used the software IBM SPSS Statistics 19 and Analyse-it V2.22 to analyse the data after all the values were compiled. The data was analyzed in two parts including curves of every volunteer and a statistics analysis. Every part we took from four areas including circumferential shortening (CS), radial shortening (RS), longitudinal shortening (LS) and rotation to detect the effect on the heart with different doses of Esmolol. And for Statistics analysis, we separated each area into four

directions including maximum of myocardial shortening, area under the curve (AUC), time to myocardial maximum movement and upslope (the speed of myocardial contraction).

Result: The typical curves of the results show that with lower doses of Esmolol (5, 10, 25 µg/kg/min), the CS, RS, LS and rotation are enhanced in comparison to higher doses and without Esmolol. In most volunteers a shift of shortening curves towards earlier heart phases and a decrease in AUC became visible. Lower doses of β-blockers induced a shortened and stronger systole while ventricular work decreased. For statistics analysis, the results of each part (CS, RS, LS and rotation) are almost the same.

Myocardial Maximum movement: from dose 5 to 25 µg/kg/min, the medians and means are higher than the dose 0µg/kg/min. But from dose 50µg/kg/min the line bends downwards.

Time to myocardial maximum movement: the time of contraction to maximum in circumference becomes shorter when Esmolol is injected with a dose of 5 µg/kg/min. When we injected 10µg/kg/min, the time to the maximum contraction reduces most. From dose 25 µg/kg/min the time line rises. The time in doses of 50, 100, 150 µg/kg/min is longer than the lower three doses.

The Area under the curve (AUC): which describes the ventricular performance shows that in three lower doses 5, 10, 25 µg/kg/min the medians and means are higher than with the dose of 0 µg/kg/min. From dose 50µg/kg/min, the values are lower than with the basic dose. So it can show that within the doses 5, 10, 25 µg/kg/min the conferential shortening of myocardium is much stronger.

Upslope: with the dose of 5 and 10 µg/kg/min, the upslope for contraction speed is higher than without Esmolol and other three higher doses obviously. From dose 25 µg/kg/min, the upslope goes down.

Unfortunately, the P value of all the statistics results are >0.05 but most of the results are at a confidence interval of 95%.

Conclusion: About the mechanism of lower doses of β-blockers with better myocardial movement change, there is a trend that it is relative to different sensitivity of the differently aggregated myocytes. The oblique myocytes which generate auxotonic forces and counteract to the mural thickening are more sensitive to β-blockers than the tangential myocytes. This standpoint has also been proved by Dr. Lunkenheimer (47) neither his nor our group have detected why the oblique myocytes are more sensitive to β-blockers than the tangential myocytes. We assume this is due to the different distribution of β-receptors. Esmolol is a kind of β_1-blocker. So if there are much more β_1-receptors on oblique myocytes than on tangential myocytes, the oblique myocytes are more sensitive to lower doses of Esmolol. Our group will try to prove this in future experiments.

7 Literature

1 Lloyd-Jones D, Adams RJ, Brown TM, et al. Heart disease and stroke statistics: 2010 update: a report from the American Heart Association. Circulation 2010;121:e46-e215.

2 Gaemperli O, Liga R, Spyrou N, et al. Myocardial beta-adrenoceptor down-regulation early after infarction is associated with long-term incidence of congestive heart failure. Eur Heart J 2010;31:1722-9.

3 Sengupta PP, Krishnamoorthy VK, Korineck J, et al. Left ventricular form and function revisited: applied translational science to cardiovascular ultrasound imaging. J Am Soc Echocardiogr 2007;20:539-51.

4 Lunkenheimer PP, Redmann K, Kling N, et al. The threedimensional architecture of the left ventricular myocardium. Anat Rec A Discov Mol Cell Evol Biol 2006;288A:565-78.

5 Jin YF, Han HC, Berger J, et al. Combining experimental and mathematical modeling to reveal mechanisms of macrophage-dependent left ventricular remodeling. BMC Syst Biol 2011;5:60.

6 Babür Güler G, Karaahmet T, Tigen K. Myocardial fibrosis detected by cardiac magnetic resonance imaging in heart failure: impact on remodeling, diastolic function and BNP levels. Anadolu Kardiyol Derg 2011;1:71-6.

7 Anguita Sánchez M, Jiménez-Navarro M, Crespo M, et al. Effect of a training program for primary care physicians on the optimization of beta-blocker treatment. Rev Esp Cardiol 2010;63:677-85.

8 Flather MD, Shibata MC, Coats AJ, et al. Randomized trial to determine the effect of nebivolol on mortality and cardiovascular hospital admission in elderly patients with heart failure (SENIORS). Eur Heart J 2005;26:215-25.

9 Smith DT, Farzaneh-Far R, Ali S, et al. Relation of beta-blocker use with frequency of hospitalization for heart failure in patients with left ventricular diastolic dysfunction (from the Heart and Soul Study).Am J Cardiol 2010;105:223-8.

10 Grant RP. Notes on the muscular architecture of the left ventricle. Circulation 1965;32:301-8.

11 Dorri F, Niederer PF, Redmann K, et al. An analysis of the spatial arrangement of the myocardial aggregates making up the wall of the left ventricle. Eur JCardi-thorac Surq 2007;31:430-7.

12 Anderson RH, Ho SY, Sanchez-Quintana D, et al. Heuristic problems in defining the three-dimensional arrangement of the ventricular myocytes. Anat Rec A Discov Mol Cell Evol Biol 2006;288:579-86.

13 Lunkenheimer PP, Redmann K, Florek J, et al. The forces generated within the musculature of the left ventricular wall. Heart 2004;90:200-7.
14 Axel L, Montillo A, Kim D. Tagged magnetic resonance imaging of the heart: a survey. Med Image Anal 2005;9:376-93.
15 Zerhouni EA, Parish DM, Rogers WJ, et al. Human heart: tagging with MR imaging-a method for noninvasive assessment of myocardial motion. Radiology 1988;169:59-63.
16 Götte MJ, Germans T, Rüssel IK, et al. Myocardial strain and torsion quantified by cardiovascular magnetic resonance tissue tagging: studies in nor-mal and impaired left ventricular function. J Am Coll Cardiol 2006;21:2002-11.
17 Shehata ML, Cheng S, Osman NF, et al. Myocardial tissue tagging with cardiovascular magnetic resonance. J Cardiovasc Magn Reson 2009;11:55.
18 Rutz AK, Ryf S, Plein S, et al. Accelerated whole-heart 3D CSPAMM for myocardial motion quantification. Magn Reson Med 2008;59:755-63.
19 Gardner RS, Martin W, Carter R, et al. Importance of b blockade in the treatment of advanced heart failure. Heart 2003;89:1442-4.
20 McAlister FA, Wiebe N, Ezekowitz JA, et al. Meta-analysis: beta-blocker dose, heart rate reduction, and death in patients with heart failure. Ann Intern Med 2009;150:784-94.
21 Basile JN. Titration of beta-blockers in heart failure. How to maximize benefit while minimizing adverse events. Postgrad Med 2003;113:63-70.
22 Tandon P, McAlister FA, Tsuyuki RT, et al. The use of beta-blockers in a tertiary care heart failure clinic: dosing, tolerance, and outcomes. Arch Intern Med 2004;164:769-74.
23 Laßnig E, Auer J, Berent R, et al. Beta-blockers and heart failure. J Clin Cardiol 2001;4:11-4.
24 Mehva R, Brocks DR. Stereospecific pharmacokinetics and pharmacodynamics of beta-adrenergic blockers in humans. J Pharm Pharm Sci 2001;4:185-200.
25 Patel AR, Shaddy RE. Role of β-blocker therapy in pediatric heart failure. Ped Health 2010;4:45-58.
26 Ryf S, Schwitter J, Spiegel MA, et al. Accelerated tagging for the assessment of left ventricular myocardial contraction under physical stress. J Cardiovasc Magn Reson 2005;7:693-703.
27 Ryf S, Spiegel MA, Gerber M, et al. Myocardial tagging with 3D-CSPAMM. J Magn Reson Imaging 2002;16:320-5.
28 Lunkenheimer PP, Lunkenheimer A, Whimster WF, et al. Local myocardial and global ventricular function compared during positive inotropic medication. Basic Res Cardiol 1986;81 Suppl 1:59-71.

29 Salton CJ, Chuang ML, O'Donnell CJ, et al. Gender differences and normal left ventricular anatomy in an adult population free of hypertension. A Cardiovascular Magnetic Resonance Study of the Framingham Heart Study Offspring Cohort. J Am Coll Cardiol 2002;39:1055-60.

30 Moore CC, Lugo-Olivieri CH, McVeigh ER, et al. Three-dimensional systolic strain patterns in the normal human left ventricle: Characterization with Tagged MR Imaging. Radiology 2000;214:453-66.

31 Maier SE, Fischer SE, McKinnon SE, et al. Evaluation of left ventricular segmental wall motion in hypertrophic cardiomyopathy with myocardial tagging. Circulation 1992;86:1919-28.

32 Goffinet C, Chenot F, Robert A, et al. Assessment of subendocardial vs.subepicardial left ventricular rotation and twist using twodimensional speckle tracking echocardiography: comparison with tagged cardiac magnetic resonance. Eur Heart J 2009;30:608-17.

33 Kramer CM, Malkowski MJ, Mankad S, et al. Magnetic resonance tagging and echocardiographic response to dobutamine and functional improvement after reperfused myocardial infarction. Am Heart J 2002;143:1046-51.

34 Nagel E, Lehmkuhl HB, Bocksch W, et al. Noninvasive diagnosis of ischemia-induced wall motion abnormalities with the use of high-dose dobutamine stress MRI comparison with dobutamine stress echocardiography. Circulation 1999;99:763-70.

35 Masood S, Yang GZ, Pennell DJ, et al. Investigating intrinsic myocardial mechanics: the role of MR tagging, velocity phase mapping, and diffusion imaging. J Magn Reson Imaging 2000;12:873-83.

36 Kramer U, Deshpande V, Fenchel M, et al. Cardiac MR tagging: optimization of sequence parameters and comparison at 1.5 T and 3.0 T in a volunteer study. Rofo 2006;178:515-24.

37 Fischer SE, McKinnon GC, Maier SE, et al. Improved myocardial tagging contrast. Magn Reson Med 1993;30:191-200.

38 Castillo E, Lima AC, Bluemke DA. Regional myocardial function: advances in MR Imaging and analysis. Radiographics 2003;23:S127-40.

39 Markl M, Schneider B, Hennig J. Fast phase contrast cardiac magnetic resonance imaging: improved assessment and analysis of left ventricular wall motion. J Magn Reson Imaging 2002;15:642-53.

40 Garot J, Bluemke DA, Osman NF, et al. Fast determination of regional myocardial strain fields from tagged cardiac images using harmonic phase MRI. Circulation 2000;101:981-8.

41 Osman NF, Kerwin WS, McVeigh ER, et al. Cardiac motion tracking using CINE harmonic phase (HARP) magnetic resonance imaging. Magn Reson Med 1999;42:1048-60.

42 de Boer RA, Voors AA, Van Veldhuisen DJ. Nebivolol: third generation beta-blockade. Expert Opin Pharmacother 2007;8:1539-50.

43 Wikstrand J, Kendall M. The role of beta receptor blockade in preventing sudden death. Eur Heart J 1992;13Suppl D:111-20.

44 Alexander R, Binns J, Hetreed M. A controlled trial of the effects of esmolol on cardiac function. Br J Anaesth 1994;72:594-5.

45 Boldt J, Suttner S. Combined use of ultra-short acting beta-blocker esmolol and intravenous phosphodiesterase 3 inhibitor enoximone. Expert Opin. Pharmacother 2007;8:2135-47.

46 Klein G, Wirtzfeld A, Alt E, et al. Antiarrhythmic activity of esmolol (ASL-8052)-a novel ulra-short acting beta-adrenoreceptor blocking agent. Int J Clin Pharmacol Ther Toxicl 1984;22:112-7.

47 Lunkenheimer PP, Redmann K, Cryer CW, et al. Beta-blockade at low doses restoring the physiological balance in myocytic antagonism. Eur J Cardiothorac Surg 2007;32:225-30.

48 Bristow MR, Ginsburg R, Umans V, et al. Beta1- and beta2-adrenergic-receptor subpopulations in nonfailing and failing human ventricular myocardium: coupling of both receptor subtypes to muscle contraction and selective beta 1-receptor down- regulation in heart failure. Circulation Research 1986;59:297-309.

49 Viskin S, Kitzis I, Lev E, et al. Treatment with beta-adrenergic blocking agents after myocardial infarction: from randomized trials to clinical practice. J Am Coll Cardiol 1995;25:1327-32.

50 Rochon PA, Tu JV, Anderson GM, et al. Rate of heart failure and 1-year survival for older people receiving low-dose beta-blocker therapy after myocardial infarction. Lancet 2000;356: 639-44.

51 Baxter AJ, Spensley A, Hildreth A, et al. Beta blockers in older persons with heart failure: tolerability and impact on quality of life. Heart 2002;88:611-4.

52 Dobre D, DeJongste MJ, Lucas C, et al. Effectiveness of β-blocker therapy in daily practice patients with advanced chronic heart failure; is there an effect-modification by age? Br J Clin Pharmacol 2006;63:356-64.

53 Bristow MR, O'Connell JB, Gilbert EM, et al. Dose-response of chronic beta-blocker treatment in heart failure from either idiopathic dilated or ischemic cardiomyopathy. Bucindolol investigators. Circulation 1994;89:1632-42.

54 Felix SB, Stangl V, Kieback A, et al. Acute hemodynamic effects of β-blockers in patients with severe congestive heart failure: comparison of celiprolol and esmolol. J Cardiovasc Pharmacol 2001;38:666-71.

55 Wikstrand J, Hjalmarson A, Waagstein F, et al. Dose of Metoprolol CR/XL and clinical outcomes in patients with heart failure. Analysis of the experience in Metoprolol CR/XL randomized intervention trial in chronic heart failure (MERIT-HF). J Am Coll Cardiol 2002;40:491-8.

56 Barron HV, Viskin S, Lundstrom RJ, et al. Beta-blocker dosages and mortality after myocardial infarction. Arch Intern Med 1998;158:449-53.

57 Ho KK, Anderson KM, Kannel WB, et al. Survival after the onset of congestive heart failure in Framingham Heart Study subjects. Circulation 1993;88:107-115.

58 Krum H, Hill J, Fruhwald F, et al. Tolerability of beta-blockers in elderly patients with chronic heart failure: The COLA II study. Eur J Heart Fail 2006;8:302-7.

59 Simon T, Mary-Krause M, Funck-Brentano C, et al. Bisoprolol dose–response relationship in patients with congestive heart failure: a subgroup analysis in the cardiac insufficiency bisoprolol study (CIBIS II). Eur Heart J 2003;24:552-9.

60 Dulin BR, Haas SJ, Abraham WT, et al. Do elderly systolic heart failure patients benefit from beta blockers to the same extent as the non-elderly? Meta-analysis of > 12,000 patients in large-scale clinical trials. Am J Cardiol 2005;95:896-8.

61 Raza JA, Movahed A. Use of cardiovascular medications in the elderly. Int J Cardiol 2002;85:203-15.

62 Loyer X, Oliviero P, Damy T, et al. Effects of sex differences on constitutive nitric oxide synthase expression and activity in response to pressure overload in rats. Am J Physiol Heart Circ Physiol 2007;293:H2650-8.

63 Mills PJ, Ziegler MG, Nelesen RA, et al. The effects of the menstrual cycle, race, and gender on adrenergic receptors and agonists. Clin Pharmacol Ther 1996;60:99-104.

64 Luzier AB, Killian A, Wilton JH, et al. Gender-related effects on metoprolol pharmacokinetics and pharmacodynamics in healthy volunteers. Clin Pharmacol Ther 1999;66:594-601.

65 Simon T, Mary-Krause M, Funck-Brentano C, et al. Sex differences in the prognosis of congestive heart failure results from the cardiac insufficiency Bisoprolol Study (CIBIS II). Circulation 2001;103:375-80.

66 Ghali JK, Krause-Steinrauf HJ, Adams KF, et al. Gender differences in advanced heart failure: insights from the BEST study. J Am Coll Cardiol 2003;42:2128-34.

67 Packer M, Bristow MR, Cohn JN, et al. The effect of carvedilol on morbidity and mortality in patients with chronic heart failure. N Engl J Med 1996;334:1349-55.

68 Ghali JK, Piña IL, Gottlieb SS, et al. Metoprolol CR/XL in female patients with heart failure analysis of the experience in metoprolol extended-release randomized intervention trial in heart failure (MERIT-HF). Circulation 2002;105:1585-91.

69 MERIT-HF Study Group. Effect of metoprolol CR/XL in chronic heart failure: Metoprolol CR/XL randomised intervention trial in congestive heart failure. Lancet 1999;353:2001-7.

70 Levy D, Savage DD, Garrison RJ, et al. Echocardiographic criteria for left ventricular hypertrophy: the Framingham Heart Study. Am J Cardiol 1987;59:956-60.

8 Figure List

Fig.1.2.1a-b The reconstruction of the left ventricle ---- 4
Fig.1.2.2.a The changing of the long axis of the aggregated myocytes ---- 5
Fig.1.2.2.b The variation in angles of the long axis of the aggregated myocytes ---- 5
Fig.1.2.3 Realignment of an aggregate of myocytes from diastole to systole ---- 7
Fig.1.2.4 The orientations of aggregated myocytes from the base to apex of heart ---- 7
Fig.1.2.5.a The arrangement of the fibrous tissue of the heart ---- 8
Fig.1.2.5.b Fibrous matrix of the ventricular myocytes by histological section ---- 8
Fig.1.3.1 Basic principle of myocardial magnetic resonance tagging ---- 9
Fig.3.6.1 Menus of software TagTrack ---- 19
Fig.3.6.2 Myocardial tagging on a short axis image over 24 phases ---- 20
Fig.3.6.3 Myocardial tagging on a long axis image over 24 phases ---- 20
Fig.3.6.4 Statistic of Myocardial Tagging on circumferential shortening ---- 21
Fig.4.a-b Figures of tagged myocardium for circumferential and longitudinal shortening ---- 22
Fig.4.1.a Post-processed slicewise resulting in a value for different shortening and rotation ---- 23
Fig.4.1.b The Maximum movement of myocardium, Time to maximum, AUC and Upslope ---- 23
Fig.4.1.1.a-c Typical curves of circumferential shortening derive from 3D myocardial tagging data with different doses of Esmolol ---- 24
Fig.4.1.2 The movement of myocardium in radial shortening with different doses of Esmolol ---- 25
Fig.4.1.3 The rotation of the heart with different doses of Esmolol ---- 26
Fig.4.1.4 The curves of longitudinal shortening with different doses of Esmolol ---- 27
Fig.4.2.1.1 The maximum movement of myocardium in CS with different doses of Esmolol ---- 28
Fig.4.2.1.2 The AUC in CS with different doses of Esmolol ---- 28
Fig.4.2.1.3 The time of maximum movement in CS with different doses of Esmolol ---- 29
Fig.4.2.1.4 The upslope of CS with different doses of Esmolol ---- 30
Fig.4.2.2.1 The maximum movement of myocardium in RS with different doses of Esmolol ---- 31
Fig.4.2.2.2 The AUC in RS with different doses of Esmolol ---- 31
Fig.4.2.2.3 The time of maximum movement in RS with different doses of Esmolol ---- 32
Fig.4.2.2.4 The upslope of RS with different doses of Esmolol ---- 33
Fig.4.2.3.1 The maximum movement of myocardial in ROT with different doses of Esmolol ---- 33
Fig.4.2.3.2 The AUC in ROT with different doses of Esmolol ---- 34
Fig.4.2.3.3 The time of maximum movement in ROT with different doses of Esmolol ---- 35
Fig.4.2.3.4 The upslope of ROT with different doses of Esmolol ---- 35
Fig.4.2.4.1 The maximum movement of myocardium in LS with different doses of Esmolol ---- 36
Fig.4.2.4.2 The AUC in LS with different doses of Esmolol ---- 37
Fig.4.2.4.3 The time of maximum movement in LS with different doses of Esmolol ---- 37
Fig.4.2.4.4 The upslope of LS with different doses of Esmolol ---- 38

9 Curriculum Vitae

Mein Lebenslauf wird aus datenschutzrechtlichen Gründen in der elektronischen Version meiner Arbeit nicht veröffentlicht.

10 Statement in lieu of oath

This dissertation is the result of my own work and has not been created with the prohibited help of others. I have neither used further material nor the words of authors other than quoted. All quotes that were literally or in their sense taken from published or unpublished sources as well as oral information are clearly identified as such.

I hereby declare that this thesis has solely been composed by me without the help of others unless stated otherwise and that no direct or indirect payment has been made to third parties.

This thesis has not been submitted in this or in similar form to any national or international institution as dissertation or for any other degree.

This is my first attempt in submitting a dissertation.

Berlin, 04.12.2012

_____

(Tieyan Li / 李铁岩)

11 Acknowledgement

During the whole thesis, many teachers and my colleagues helped me a lot. Thus on behalf of myself and my family, I would like to thank a lot and express my sincere appreciation to my supervisor Prof. Dr. med. Felix Berger for offering the opportunity and providing support to carry out this study in the department of congenital heart disease and paediatric cardiology in the Deutsches Herzzentrum Berlin, and for his continuous guidance, encouragement and care throughout the entire period of the study. Also his critical reading of this manuscript and insight and thoughtful comments are highly appreciated.

I would also like to express my sincere gratitude to my tutor Dr. med. Boris Schmitt for leading me to the scientific research field, for his constructive and helpful directions throughout the entire period of study, and for his critical reading and revision.

I am very grateful to Katharina Weber for her English correction of my thesis and help all the time. Also I would express my thanks to Stefan Schröder for his support and help in daily affairs. Further I want to thank Marco Bartosch for his reading and correction of my thesis. I am also very grateful to Katharina Dauenhauer, Hendrik Spriestersbach, Antonia Prudlo for their assistance in the whole study. I also thank Prof. Dr. med. Titus Kühne for his help.

Furthermore I would like to show my thanksgiving and appreciation to Prof. Dr. med. Yuguo Weng and Prof. Dr. med. Zhongmin Liu for their help and guidance.

At last I would like show my sincere appreciation to my wife Lin Zou and my family. Thanks for their support and care all time no matter what happens.

12 Zusammenfassung

Die Muskulatur des Herzens verfügt im Vergleich zur glatten und Skelettmuskulatur über eine spezifische Anatomie und eine komplexe Architektur. Die ventrikuläre Myokardmasse ist wie ein Maschengewebe aufgebaut, besiedelt von Myozyten, die in einer unterstützenden Kollagenmatrix angeordnet sind. Die meisten Muskelfasern sind spiralig tangential angeordnet. Jedoch verlaufen Myozyten auch antagonistisch dazu schräg transmural vom Epikard zum Endokard. Wenn sich bei der Kontraktion des Herzens die ventrikuläre Wand verdickt, werden die schräg transmural angeordneten Myozyten progressiv an der Verkürzung gehindert. Die ungleichen Arbeitsbedingungen dieser tangentialen und schräg verlaufenden transmuralen Komponenten des Myokards erzeugen unterschiedliche Kräfte. Die Myozyten, deren lange Achsen quer durch die kurze Achse der Wand angeordnet sind, können auxotonische Kräfte erzeugen. Diese stehen entgegen der Kraft, die von den tangential angeordneten Myozyten erzeugt wird und wirken einer Verdickung der Ventrikelwand entgegen. Dem Design dieser Studie liegt die These zugrunde, dass diese beiden Gruppen von Myozyten zwei Arten von Kräften generieren: die erste veranlasst das Zusammenziehen des Myokards, die andere wirkt der Verdickung des Ventrikels entgegen. Untersucht wurden verschiedene Dosen von β-Blockern mit Kurzzeitwirkung hinsichtlich ihres Effektes auf die Myozyten und die Funktion des Myokards mit Hilfe einer MRT-Tagging-Methode.

MRT-Tagging ist eine gängige Methode auf Basis der Magnetresonanz, um die Herzfunktion zu untersuchen sowie Besonderheiten der Myokardverformung zu erkennen. Es ist ein integrierter Ansatz, der schnelle Aufnahmen von Pulssequenzen in allen drei Raumrichtungen zur gleichen Zeit, ein gemeinsames Elektrokardiogramm (EKG) und Atemtriggerung kombiniert. Parallele Bildgebung und spezielle kardiale Spulen konnten 3D-Tagging klinisch praktikabel machen.

Complementary Spatial Modulation of Megnetization (CSPAMM) ist eine der MRT-Tagging-Technologien, die das Verlöschen der Markierungen (Tags) durch T1-Relaxation minimieren kann und die auch das Markieren (Taggen) und Beurteilen des ganzen Herzens zulässt. Es ist eine sehr genaue Messmethode, um regionale Kontraktions- und Relaxionsmuster des Myokards im gesunden oder erkrankten Herzen zu beurteilen. Desweiteren ist MRT-Tagging durch die große Menge von Tagging-Daten sehr präzise. So kann der transmurale Belastungsgradient aufgezeigt werden. Auch ist es durch seine Symmetrie in der umlaufenden und vertikalen Achse in der Lage, örtliche Veränderungen der Faserwinkel aufzuspüren. Aufgrund der Vorteile des MRT-Taggings, die Funktion des Myokards darzustellen, wurde diese Methode gewählt.

In unserer Studie wurden 13 Probanden untersucht, freiwillige Studienteilnehmer (6 weiblich, 7 männlich) aus Berlin mit einem Durchschnittsalter von 36 Jahren (von 29 bis 41 Jahren). Alle Versuchsteilnehmer gaben eine Einverständniserklärung und unterzogen sich vor der Behandlung einer körperlichen Untersuchung. Während der gesamten Prozedur wurde bei allen Probanden alle 3 Minuten EKG, Blutdruck und SpO2 überwacht. Nach der Vorbereitung und Lagerung im MRT bekamen alle Probanden intravenöse Injektionen von Esmolol in Dosen von 0 µg/kg/min bis 150 µg/kg/min. Die Esmolol-Dosen wurden sukzessive über einen Zeitraum von etwa 12-13 Minuten gegeben. Nach jeder Gabe wurde etwa 4 Minuten gewartet, bis die Wirkung eintrat. Dann begann der MRT-Scan. Esmolol ist ein cardio-selektiver β1-adrenerger Rezeptor-Blocker ohne signifikante intrinsische sympathomimetische Aktivität, vasodilatatorische Eigenschaften, wesentliche membran-stabilisierender Aktivität oder β2-agonistischen Effekten. Es verfügt über eine kurze Wirkeintrittszeit von zwei Minuten und eine kurze Wirkdauer mit einer Halbwertszeit von 9 Minuten.

10 bis 20 Minuten nach Beendigung der Infusion kann eine wesentliche Erholung von dem β-Blocker beobachtet werden. 30 Minuten nach Beendigung der Esmolol Infusion waren alle hämodynamischen Parameter wieder auf Vorbehandlungsniveau. Esmolol wurde bei jedem Probanden verwendet, da es eine kurze Halbwertszeit hat, gut zu kontrollieren ist und sicher verwendet werden kann.

Um die MRT-Tagging Daten auszuwerten, wurde eine Methode namens Harmonic Phase (HARP) mit einer 2D oder 3D TagTrack Software angewendet. Eine HARP Analyse ist derzeit die gängigste Methode für Verformungs-Quantifizierung, da es hoch automatisiert ist und sowohl Analysezeit als auch subjektive Interferenz limitiert. Für die statistische Auswertung der gesammelten Daten wurde die IBM Software SPSS Statistics 19 und Analyse-it V2.22 verwendet. Die Daten wurden in zwei Abschnitten analysiert: die Kurven von jedem einzelnen Probanden und eine statistischen Analyse. Jeder dieser Abschnitte wurde aus vier Kategorien ermittelt: Verkürzung des Umfangs, (circumferential shortening, CS), radiale Verkürzung (radial shortening, RS), Verkürzung der Längsachse (longitudinal shortening, LS) und Rotation (rotation) um die Auswirkungen von Esmolol auf das Herz zu ermitteln. Für die statistische Auswertung wurde jede dieser Kategorien in vier Bereiche unterteilt:

Das Verkürzungsmaximum des Myokards (MAX), die Dauer bis zur maximalen Myokardverkürzung (TTP), die Fläche unter der Kurve (area under the curve, AUC) und der Anstieg der Kurve (die Geschwindigkeit der Kontraktion des Myokards, Upslope).

Die typischen Kurven für CS, RS, LS und die Rotation zeigen, dass niedrige Dosierungen von Esmolol (5, 10, 25 μg/kg/min) im Gegensatz zu höheren Dosen das Verkürzungsmaximum und die Geschwindigkeit der Kontraktion steigern. Bei den meisten Probanden konnte eine Verlagerung der Kurven zu den frühen Herzphasen und eine Reduzierung der AUC beobachtet werden. Niedrigere Dosen von β-Blockern induzierten somit eine verkürzte und stärkere Systole, während sich die ventrikuläre Arbeitslast (AUC) reduzierte. Im Vergleich dazu verringerten höhere Dosen von β-Blockern die ventrikuläre Kontraktionsgeschwindigkeit, was eine längere Systole mit gesteigerter ventrikulärer Arbeitslast hervorrief.

In der statistischen Auswertung sind die Ergebnisse für die vier Bereiche Verkürzungsmaximum des Myokards, Fläche unter der Kurve (area under the curve, AUC), Dauer bis zur größten Bewegung des Myokards und Anstieg der Kurve (die Geschwindigkeit der Kontraktion des Myokards) für jede der vier Kategorien Verkürzung des Umfangs, (circumferential shortening, CS), radiale Verkürzung (radial shortening, RS), Verkürzung der Längsachse (longitudinal shortening, LS) und Rotation (rotation) fast gleich.

Maximale Myokardbewegung: Bei Dosen von 5 bis 25 μg/kg/min sind Mittwelwert und Median höher als bei einer Dosis von 0 μg/kg/min. Bei einer Dosis von 50 μg/kg/min hingegen, knickt die Kurve nach unten ab.

Dauer bis zur maximalen Myokardbewegung: Die Dauer der Kontraktion bis zum Maximum des Umfangs verkürzt sich bei einer Dosis von 5 μg/kg/min Esmolol. Bei einer Gabe von 10 μg/kg/min reduziert sich die Dauer bis zum Kontraktionsmaximum am stärksten. Ab einer Dosis von 25 μg/kg/min steigt die Kurve an. Die Dauer ist bei Dosen von 50, 100 und 150 μg/kg/min länger als bei den drei niedrigeren Dosen.

Die Fläche unter der Kurve (AUC): Sie beschreibt die ventrikuläre Leistung und zeigt, dass bei den niedrigeren Dosen von 5, 10 und 25 μg/kg/min Median und Mittelwert höher sind als bei einer Dosis von 0 μg/kg/min (Ausgangswert). Ab einer Dosis von 50 μg/kg/min sind die Werte niedriger als der Ausgangswert. So kann gezeigt werden, dass bei einer Dosis von 5, 10 und 25 μg/kg/min die Umfangsreduzierung des Myokards viel stärker ist.

Anstieg: Bei Dosen von 5 und 10 μg/kg/min ist der Anstieg der Verkürzungskurven als Ausdruck der Kontraktionsgeschwindigkeit höher als ohne Esmolol und als bei den anderen drei Dosen. Ab einer Dosis von 25 μg/kg/min fällt die Kurve ab.

Leider sind die P-Werte bei allen statistischen Ergebnisse >0.05, d.h. auf Basis eines Konfidenzintervalls von 95% zeigen sich keine statistischen Unterschiede zwischen den Medikamentendosierungen.

.

Nichtsdestotrotz kann diese Studie tendenziell zeigen, dass niedrigere Dosen von Esmolol im Gegensatz zu hohen Dosen die Funktion des Myokards verbessern. Die Verbesserungen der Funktion des Myokards beinhalten Zunahme der Verkürzung des transversalen Ventrikelumfanges (circumferential shortening, CS), der radialen Verkürzung (radial shortening, RS), der Verkürzung des Längsumfanges (longitudinal shortening, LS) und der Rotation (rotation).

Bezüglich der niedrigeren Dosen von Esmolol postulieren wir den Trend, dass dieses relativ zu den Esmolol-Sensibilitäten der verschieden angeordneten Myozytengruppen wirkt.

Die schräg verlaufenden Myozyten, die auxotone Kräfte generieren und gegen die systolische Wandverdickung agieren, reagieren schneller auf β-Blocker als die tangential angeordneten Myozyten, die die Mehrheit der Muskelfaserzellen darstellen und hauptsächlich für die Konstriktion des linken Ventrikels verantwortlich sind.

Diese These wurde von Dr. Lunkenherimer experimentell aufgestellt, obwohl weder er noch seine Arbeitsgruppe erkennen konnten, warum die schräg laufenden Myozyten sensitiver auf β-Blocker reagieren als die tangential verlaufenden. Wir gehen davon aus, dass dies an der unterschiedlichen Aktivität der verschieden ausgerichteten Myozytenaggregate während eines myokardialen Erregungs- und Kontraktinoszykluses liegt. Helikal verlaufende Myozyten kontrahieren überwiegend in Form einer Unterstützungszuckung. Schräg einwärts verlaufende Myozyten müssen dagegen in einer auxotonen (zu gleichen Teilen isometrischen und isotonisch) bis überwiegend isometrisch Form kontrahieren. Die Kontraktionsdauer der zweiten Myozytengruppe und somit deren ATP/cAMP- und Kalzium-Verbrauch liegt höher. Dadurch ist diese Myozytengruppe auch anfälliger für eine β-Blockade, die Bereitstellung von energiereichen Metaboliten und Kalzium reduziert. Unsere Arbeitsgruppe wird versuchen, diese Hypothese an weiteren klinischen Studien zu verifizieren und offene Fragen zu beantworten.

In klinischen Studien wird eine Behandlung mit Esmolol häufiger mit niedrigeren Dosen beschrieben, als die von uns verwendeten. Aufgrund der Tatsache, dass Patienten häufig älter und gebrechlicher sind und an Erkrankungen, (z.B. einem chronischen obstruktiven Lungenleiden) leiden, können sie die hohen Dosen von β-Blocker nicht tolerieren. Unsere Studie kommt zu dem Ergebnis, dass Kliniker ermutigt werden können, tendenziell bei Patienten niedrige Dosen von β-Blockern anzuordnen, wodurch die vorteilhaften kardialen Effekte erhalten bleiben ohne negative unerwünschte Wirkungen hervorzurufen.